Multimorph Eco-Evolutionary Dynamics in Structured Populations

Sébastien Lion,[1,*] Mike Boots,[2,3] and Akira Sasaki[4,5]

1. CEFE, CNRS, Univ. Montpellier, EPHE, IRD, Montpellier, France; 2. Integrative Biology, University of California, Berkeley, California 94720; 3. Biosciences, University of Exeter, Penryn Campus, Exeter TR10 9FE, United Kingdom; 4. Department of Evolutionary Studies of Biosystems, Graduate University of Advanced Studies, SOKENDAI, Hayama, Kanagawa 2400193, Japan; 5. Evolution and Ecology Program, International Institute for Applied Systems Analysis, Schlosplatz 1, A-2361 Laxenburg, Austria

Submitted July 9, 2021; Accepted March 1, 2022; Electronically published July 21, 2022

Online enhancements: supplemental PDF.

ABSTRACT: Our understanding of the evolution of quantitative traits in nature is still limited by the challenge of including realistic trait distributions in the context of frequency-dependent selection and ecological feedbacks. We extend to class-structured populations a recently introduced "oligomorphic approximation," which bridges the gap between adaptive dynamics and quantitative genetics approaches and allows for the joint description of the dynamics of ecological variables and of the moments of multimodal trait distributions. Our theoretical framework allows us to analyze the dynamics of populations composed of several morphs and structured into distinct classes (e.g., age, size, habitats, infection status, and species). We also introduce a new approximation to simplify the eco-evolutionary dynamics using reproductive values. We illustrate the effectiveness of this approach by applying it to the important conceptual case of two-habitat migration-selection models. In particular, we show that our approach allows us to predict both the long-term evolutionary end points and the short-term transient dynamics of the eco-evolutionary process, including fast evolution regimes. We discuss the theoretical and practical implications of our results and sketch perspectives for future work.

Keywords: quantitative genetics, adaptive dynamics, reproductive value, environmental feedbacks, timescales.

Introduction

Many experimental and empirical studies in evolutionary ecology aim at understanding how ecological processes affect how trait distributions change over time. This has motivated the development of quantitative genetics methods to analyze the dynamics of quantitative traits (Lande 1979; Bulmer 1992; Falconer 1996; Walsh and Lynch 2018). Following Lande's (1976, 1979, 1982) seminal work, most quantitative genetics models assume unimodal trait distributions and frequency-independent selection, leaving aside the problem of how multimodal distributions can be generated by frequency-dependent disruptive selection. Under these assumptions, dynamical equations for the mean and higher moments of a trait distribution can be derived for tightly clustered trait distributions (Barton and Turelli 1987, 1991; Turelli and Barton 1990). Assuming that trait distributions are narrowly localized around a single mean also allows one to incorporate frequency dependence to some extent (Iwasa et al. 1991; Abrams et al. 1993), but typically models rely on the more classical assumption that trait distributions are and remain normally distributed. However, empirical evidence of skewed (Bonamour et al. 2017) or multimodal distributions highlight the need for an alternative approach.

A major limitation of current quantitative genetics theory is the reliance on simplified ecological scenarios that are not representative of the complexity of eco-evolutionary feedbacks in nature. This led to the development of adaptive dynamics theory, which, under the assumption that evolution is limited by rare mutations, provides a mathematical framework to study the interplay between ecological and evolutionary processes (Metz et al. 1992, 1996; Dieckmann and Law 1996; Geritz et al. 1998). Many authors have noted the similarities and subtle differences between adaptive dynamics and quantitative genetics approaches under the assumptions of small mutational steps and narrow trait distributions, respectively (Abrams et al. 1993; Abrams 2001; Day 2005; Lion 2018*c*). However, there is a clear conceptual gap in the canonical approaches to adaptive dynamics and

* Corresponding author; email: sebastien.lion@cefe.cnrs.fr.

ORCIDs: Lion, https://orcid.org/0000-0002-4081-0038; Boots, https://orcid.org/0000-0003-3763-6136; Sasaki, https://orcid.org/0000-0003-3582-5865.

quantitative genetics: while adaptive dynamics has been successful in taking into account environmental feedbacks and the emergence of polymorphism under frequency-dependent disruptive selection, it does so by assuming strong constraints on the mutation process and standing variation in the population. Recently, Sasaki and Dieckmann (2011) proposed an alternative "oligomorphic approximation" to bridge the gap between adaptive dynamics and quantitative genetics theory. The crux of the approach is to decompose a multimodal trait distribution into a sum of narrow unimodal morph distributions and to derive the dynamics of the frequency, mean trait value, and variance of each morph. Suitable moment closure approximations at the morph level yield a closed dynamical system. As such, this framework can be seen as an extension of quantitative genetics theory to take into account eco-evolutionary feedbacks and polymorphic trait distributions.

The theoretical developments of Sasaki and Dieckmann (2011) rely on a number of additional assumptions, notably single-locus haploid genetics, large populations sizes, and unstructured populations. In this article, we retain the first two assumptions but investigate how class structure affects the dynamics of quantitative trait distributions. As class structure is ubiquitous in biological populations, this is an important extension to Sasaki and Dieckmann's (2011) theory, allowing us to apply the method to the majority of populations where individuals can be in distinct demographic, physiological, or ecological states, such as different age groups, developmental stages, infection status, or habitats.

The article is organized as follows. We first give a general decomposition of the trait distribution into different morphs in a population structured into distinct classes. We then show how, by assuming that each morph distribution is clustered around the morph mean, we can derive equations for the dynamics of class-specific morph frequencies, morph means, and morph variances using Taylor approximations of the vital rates describing between-class transitions. We also apply recent theory on reproductive value (Lion 2018*a*, 2018*b*; Lion and Gandon 2021) to simplify the morph dynamics at the population level. As in classical theory (Fisher 1930; Taylor 1990; Lehmann and Rousset 2014; Gardner 2015), a morph's reproductive value is a measure of how well individuals of that morph in a given class transmit their genes to future generations, and we show that it can be used as a weight to calculate the net effect of selection on a given morph. Finally, we derive some simpler results for the important limit case of two-class models and apply this general framework to three specific models describing the interplay between migration and selection in a population distributed over two habitats of distinct qualities coupled by migration. The first example revisits the local adaptation models analyzed by Meszéna et al. (1997), Ronce and Kirkpatrick (2001), Débarre et al. (2013), and Mirrahimi and Gandon (2020), but our approach allows us to express these previous results in terms of the reproductive values of each habitat and to take into account habitat-specific mutation. The second example is a two-habitat extension of the resource competition model analyzed by Sasaki and Dieckmann (2011) and highlights how our framework can shed light on frequency dependence and disruptive selection. The third example is a resource-consumer model and is used to show that our approach allows us to analyze transient eco-evolutionary dynamics fueled by nonnegligible standing variation at the population level. Together, these examples illustrate the potential of the approach in a wide range of fundamental eco-evolutionary scenarios.

Densities and Trait Distributions

We consider a population of individuals characterized by a continuous phenotypic trait. The total density of individuals with trait value z at time t is $n(z,t)$, and for simplicity we denote the total density of individuals as $n(t) = \int n(z,t)\,\mathrm{d}z$ (with a slight abuse of notation). We further assume that the population is structured into K discrete classes, which can, for instance, represent different age groups, developmental stages, or habitats. The density of individuals with trait value z in class k at time t is $n^k(z,t)$. Similarly, we write $n^k(t) = \int n^k(z,t)\,\mathrm{d}z$ for the total density of individuals in class k at time t. See table 1 for a description of the main notations in the article.

Full Distributions

The within- and across-class densities represent the raw statistics of the model. They can be used to define some useful distributions to analyze the eco-evolutionary dynamics of the population. At the ecological level, the class distribution can be defined as

$$f^k(t) = \frac{n^k(t)}{n(t)}, \tag{1}$$

which represents the fraction of individuals that are in class k at time t. Note that $\sum_k f^k(t) = 1$, where the summation is over all classes, that is, $1 \le k \le K$ (for simplicity, all summation limits will be implicit in this article).

At an evolutionary level, two trait distributions can be defined. The within-class trait distribution is

$$\phi^k(z,t) = \frac{n^k(z,t)}{n^k(t)}, \tag{2}$$

which is the frequency of individuals with trait z in class k at time t. Averaging over classes yields the across-class trait distribution

$$\phi(z,t) = \frac{n(z,t)}{n(t)}. \tag{3}$$

Table 1: Definition of mathematical symbols used in the text

Symbol	Definition	Description
$n^k(z,t)$	…	Density of individuals with trait z in class k at t
$n^k(t)$	…	Total density of individuals in class k at t
$n(z,t)$	$= \sum_k n^k(z,t)$	Density of individuals with trait z at t
$n(t)$	$= \sum_k n^k(t)$	Total density of individuals at t
$f^k(t)$	$= n^k(t)/n(t)$	Fraction of individuals in class k at t
$\phi^k(z,t)$	$= n^k(z,t)/n^k(t)$	Frequency of trait z in class k at t
$\phi(z,t)$	$= n(z,t)/n(t)$	Total frequency of trait z at time t
$f_i^k(t)$	…	Morph frequencies within class k at t
$\phi_i^k(z,t)$	…	Morph distributions within class k at t
$\bar{z}^k(t)$	$= \int z\phi^k(z,t)\,\mathrm{d}z$	Mean trait value in class k at t
$\bar{z}(t)$	$= \int z\phi(z,t)\,\mathrm{d}z$	Mean trait value at t in the whole population
$\bar{z}_i^k(t)$	$= \int z\phi_i^k(z,t)\,\mathrm{d}z$	Mean trait value of morph i in class k at t
$V^k(t)$	$= \int [z-\bar{z}^k(t)]^2\phi^k(z,t)\,\mathrm{d}z$	Trait variance in class k at t
$V(t)$	$= \int [z-\bar{z}(t)]^2\phi(z,t)\,\mathrm{d}z$	Trait variance at t in the whole population
$V_i^k(t)$	$= \int [z-\bar{z}_i{}^k(t)]^2\phi_i^k(z,t)\,\mathrm{d}z$	Morph variance in class k at t
$u_i^k(t)$	…	Frequency of class k individuals among morph i individuals
$v_i^k(t)$	…	Morph-specific individual reproductive values in class k
$c_i^k(t)$	$= v_i^k(t)u_i^k(t)$	Morph-specific class reproductive values in class k
$\phi^i(z,t)$	$= \sum_k \phi_i^k(z,t)u_i^k(t)$	Morph distribution at the population level at t (with moments $\bar{z}_i, V_i, \ldots$)
$\tilde{\phi}_i(z,t)$	$= \sum_k \phi_i^k(z,t)c_i^k(t)$	Reproductive value–weighted morph distribution at the population level at t (with moments $\tilde{z}_i, \tilde{V}_i, \ldots$)
$\mathbf{R}(z)$	…	Matrix of transition rates $r^{kj}(z)$ $(1 \le k, j \le K)$
$\bar{\mathbf{R}}$	…	Matrix of average transition rates $\bar{r}^{kj}$
$\bar{\mathbf{R}}_i$	…	Matrix of morph-i average transition rates $\bar{r}_i^{kj}$

It is easy to check that, as expected, $\int \phi^k(z,t)\,\mathrm{d}z = \int \phi(z,t)\,\mathrm{d}z = 1$. Note that the class and trait distributions are linked through the relationship $\phi(z,t) = \sum_k \phi^k(z,t)f^k(t)$.

Multimorph Decomposition

Up to now, we have made no assumption about the trait distribution in the population. With the notations defined so far, it is straightforward to produce a continuous-trait version of the Price equations derived in Lion (2018*a*), but our aim here is slightly different because we want to make specific predictions about the dynamics of multimodal distributions. Following Sasaki and Dieckmann (2011), we therefore assume that the trait distribution can be decomposed into M morphs. Specifically, we use the term "morph" to describe a cluster of continuous variants around a phenotypic mean trait. We allow morphs to have distinct distributions in different classes and write the within-class trait distributions as a mixture of morph distributions:

$$\phi^k(z,t) = \sum_i \phi_i^k(z,t)f_i^k(t), \tag{4}$$

where $\phi_i^k(z,t)$ is the distribution of morph i in class k at time t and $f_i^k(t)$ is the frequency of morph i in class k. Note that $\int \phi_i^k(z,t)\,\mathrm{d}z = 1$ and $\sum_i f_i^k(t) = 1$, where the summation is implicitly over all morphs (i.e., $1 \le i \le M$). Equation (4) is a class-specific version of equation (5) in Sasaki and Dieckmann (2011). Biologically, it means that the full distribution $\phi_k(z,t)$ can be decomposed into a sum of morph distributions, $\phi_i^k(z,t)$, each weighted by the morph frequency, $f_i^k(t)$. Figure 1 gives a graphical illustration of the multimorph decomposition using simulation results from a two-class, two-morph example (e.g., example 1 below).

Intuitively, it makes sense to associate the distribution $\phi_i^k(z,t)$ to one "peak" of a multimodal distribution, but it is important to note that the decomposition (4) is also valid if the morph distributions overlap or are similar. We can, for instance, start with two very similar morphs and study how disruptive selection causes the unimodal distribution $\phi_k(z,t)$ to split into two peaks as the morph means move away from each other. Our theoretical framework therefore does not require the distance between morph means to be large. Similarly, our analysis does not require a morph to have the same distribution or the same frequency in all classes, although it will often make biological sense to consider scenarios where the trait distributions in the different classes look similar (without being identical). Finally, while

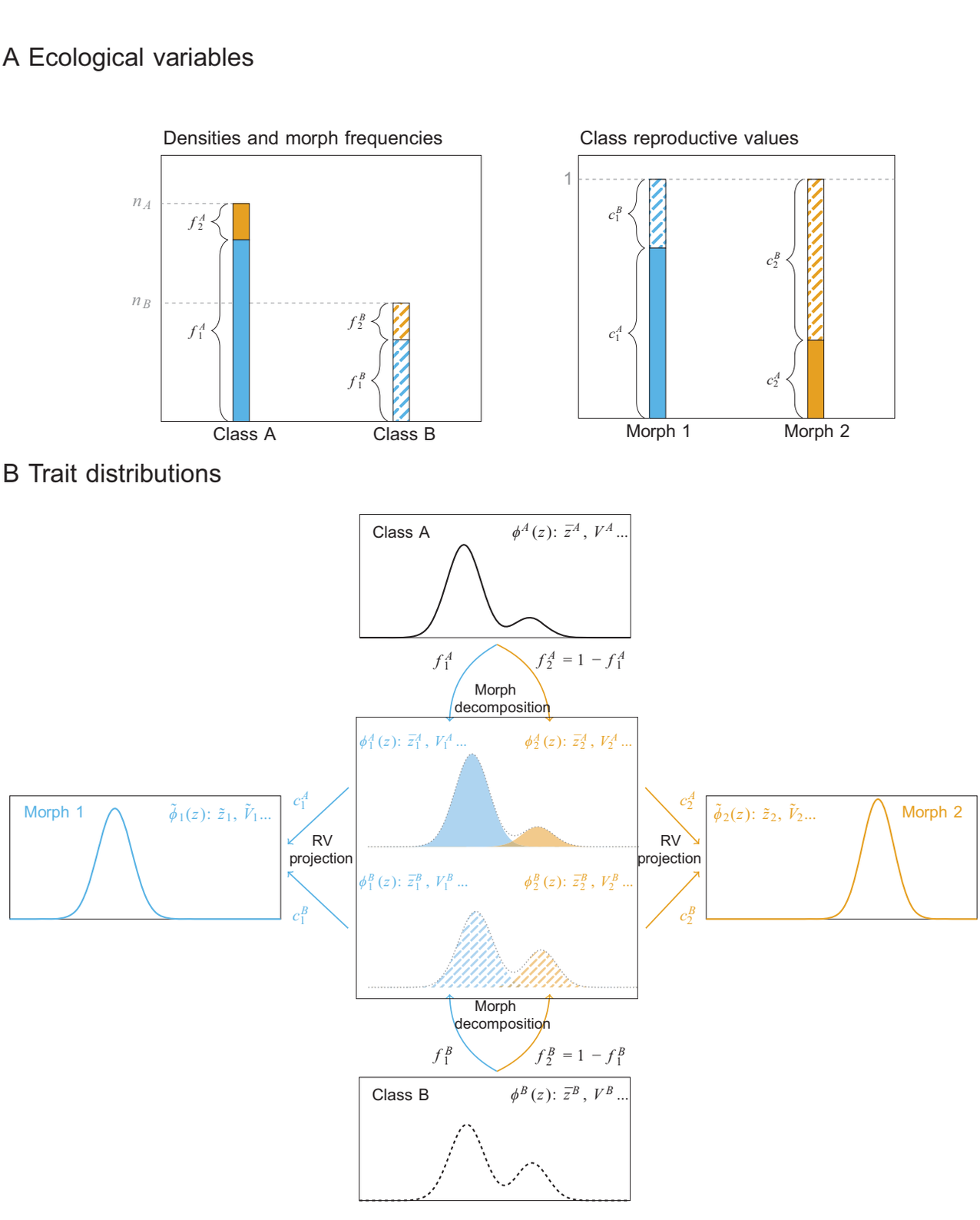

Figure 1: Summary of the notations and approach using a two-class, two-morph example. *A* shows the fast variables, which change on the ecological timescale. These are the densities of individuals in each class, $n^A(t)$ and $n^B(t)$; the morph frequencies in each class, $f_i^k(t)$; and the morph-specific class reproductive values, $c_i^k(t)$. In the simulation snapshot used to plot these graphs, morph 1 is relatively more abundant within class B ($f_1^B > f_2^B$) but has a lower class reproductive value ($c_1^B < c_2^B$). *B* shows the trait distributions, which change on the slow

the number of morphs can be arbitrarily chosen, it makes sense to use biological intuition to guide this choice (e.g., two morphs for a two-resource model; for a more formal argument, see "Discussion").

Morph Moments

From the distributions $\phi_k(z,t)$, we can calculate class-specific moments, such as $\bar{z}^k(t)$, the mean trait value in class k at time t, and $V^k(t)$, the trait variance in class k at time t. Similarly, morph-specific moments can be calculated from the distributions $\phi_i^k(z,t)$. For instance, the mean trait value of morph i in class k at time t is $\bar{z}_i^k(t)$, and the trait variance of morph i in class k at time t is $V_i^k(t)$.

If higher-order moments are negligible or can be approximated using moment closure approximations at the morph level, a morph can then be characterized by its relative abundance (e.g., its frequency in each class, f_i^k), its position (e.g., the class-specific morph mean $\bar{z}_i^k$), and its width (e.g., the class-specific morph standard deviation $\sqrt{V_i^k}$). Equation (4) allows us to make connections between population-level moments and morph-specific moments. See table 1 for explicit definitions of the population-level and morph-specific moments as well as figure 1 for a graphical summary of the notations.

Notational Conventions

To simplify the notations, a number of conventions will be used throughout the article. First, classes will be identified by superscripts and morphs by subscripts. For classes, we use the superscripts j and k, so that an implicit summation over k means that k takes values between 1 and K. For morphs, we use the subscript i, which thus takes values between 1 and M. The symbol ℓ will be used for either classes or morphs, when needed. Second, whenever it is clear from the context, we shall drop the dependency on time, writing, for example, f^k instead of $f^k(t)$.

Dynamics and Separation of Timescales

Having defined the statistics we need to describe the state of the population at a given time, we now turn to their dynamics. Figure 1 illustrates how a multimodal trait distribution can be decomposed into a mixture of unimodal morph distributions. By tracking the dynamics of these morph distributions, we can understand how the various peaks of the multimodal distribution move and change over time. To derive these dynamics, we first specify the rates associated with the different events of the life cycle, then we calculate an approximation of these rates under the assumption that the morph distributions are sufficiently narrow.

Vital Rates

At a general level, the vital rates are defined by functions $r^{jk}(z,E(t))$, which give the rate of production of individuals in class j by an individual in class k with trait z at time t. The variable $E(t)$ represents the environmental feedback, which collects all ecological variables needed to calculate the reproduction and survival of individuals (Metz et al. 1992, 2008; Mylius and Diekmann 1995; Lion 2018*c*). For clonally reproducing organisms, this is sufficient to calculate the dynamics of the density $n^j(z,t)$, as follows:

$$\frac{\mathrm{d}n^j(z)}{\mathrm{d}t} = \sum_k r^{jk}(z,E(t))n^k(z). \tag{5}$$

Equation (9) describes the interplay of selection and ecological dynamics under the assumption of perfectly faithful reproduction (i.e., individuals with trait z give birth to individuals with trait z). In our initial presentation, we find it easier to omit the mutation process, but we will consider the effect of mutation at a later stage. In addition, we do not explicitly model class-specific traits in this article (but for how this can be taken into account, see "Discussion").

In the remainder of the article, all operations on the vital rates $r^{jk}(z,E(t))$ will be partial derivatives or integration with respect to the first argument. Hence, we shall drop the dependency on environmental feedback and write simply $r^{jk}(z)$ (and $\mathbf{R}(z)$ for the matrix of vital rates). However, it must be kept in mind that this notation does not imply density-independent or frequency-independent selection. As shown in the "Applications" section, our formalism can be readily applied to scenarios where the vital rates depend on the density of conspecifics or other species, on the trait distribution, or on other biotic or abiotic ecological variables (see, e.g., Sasaki and Dieckmann 2011; Lion 2018*c*).

Small Morph Variance Approximation

The crux of the oligomorphic approximation of Sasaki and Dieckmann (2011) is to assume that the morph distributions are tightly clustered around their mean; that is, the standard deviation of the morph distribution is proportional

evolutionary timescales. The trait distribution in class A, $\phi^A(z,t)$, can be decomposed into a mixture of class-specific morph distributions, $\phi_i^A(z,t)$, weighted by the class-specific morph frequencies $f_i^A(t)$. Note that to better illustrate the decomposition, the shaded areas represent $f_i^k(t)\phi_i^k(z,t)$ and not the distributions $\phi_i^k(z,t)$. This multimorph decomposition can also be applied to class B. On the slow timescale, the relevant aggregate distributions at the morph level are the reproductive value–weighted morph distributions $\tilde{\phi}_i(z,t)$. Note that the graphs use data from a numerical simulation of example 1. RV = reproductive value.

to a small parameter ε. In a class-structured model, this means that the quantity $\xi_i^k = z - \bar{z}_i^k$ is small, and we write $\xi_i^k = O(\varepsilon)$. A simple Taylor expansion of the vital rates $r^{jk}(z)$ around the within-class morph mean $\bar{z}_i^k$ yields

$$r^{jk}(z) = r^{jk}(\bar{z}_i^k) + \xi_i^k \frac{\partial r^{jk}}{\partial z}\bigg|_{z=\bar{z}_i^k} + \frac{1}{2}(\xi_i^k)^2 \frac{\partial^2 r^{jk}}{\partial z^2}\bigg|_{z=\bar{z}_i^k} + O(\varepsilon^3). \tag{6}$$

Integrating over the distribution $\phi_i^k(z)$ yields an approximation for the average vital rates of morph i in terms of the morph-specific mean and variances $\bar{z}_i^k$ and V_i^k. We have

$$\bar{r}_i^{jk} = r^{jk}(\bar{z}_i^k) + \frac{1}{2} V_i^k \frac{\partial^2 r^{jk}}{\partial z^2}\bigg|_{z=\bar{z}_i^k} + O(\varepsilon^4). \tag{7}$$

Similarly, averaging $r^{jk}(z)$ over the distribution $\phi^k(z)$ yields the average vital rates $\bar{r}^{jk}$, which can be decomposed in terms of morph averages as $\bar{r}^{jk} = \sum_i \bar{r}_i^{jk} f_i^k$. Note that, as in Sasaki and Dieckmann (2011), we assume that the morph distributions are symmetric around their means throughout this article (which is why the remainder in eq. [7] is of order ε^4).

Separation of Timescales

Because we assume that within-morph variation is small, the oligomorphic approximation gives rise to a separation of timescales between ecological and evolutionary variables. Specifically, the dynamics of the densities n^k, class frequencies f^k, and morph frequencies f_i^k are all $O(1)$ so that these can be treated as fast variables. On the other hand, the dynamics of morph means and variances will tend to vanish as ε tends toward zero, so the morph moments change on slower timescales. It is important to realize that this does not mean that there is no feedback between ecology and evolution, and in fact this approximation can be used to study situations where rapid evolution is fueled by a large standing variance at the population level (e.g., if we have two morphs with very different mean trait values) while assuming that the standing variation in each morph remains small. This will be explored in our example 3 below.

Thus, the resulting coupled dynamics of densities, morph frequencies, morph means, and morph variances take the form of a fast-slow dynamical system (for an ecologically oriented overview, see Rinaldi and Scheffer 2000). There are two ways to interpret this system. First, it can be viewed as an approximation of the full eco-evolutionary dynamics and can be either numerically explored or used to gain analytical insight into the transient and long-term dynamics of the ecological and evolutionary variables, as is typically carried out in quantitative genetics approaches. Second, it can be analyzed using quasi-equilibrium approximations, following the typical practice in evolutionary invasion analyzes such as adaptive dynamics. This dictates that one first derive the equilibrium of the ecological variables and morph frequencies for fixed values of the morph means and variances and then use this information to calculate the dynamics of the morph means, the evolutionary singularities, and the dynamics of morph variances near these singularities.

In the following, we first derive the equations of the fast variables (the densities and morph frequencies), then those of the slow variables (the morph means and variances). This allows us to clarify the connections with previous approaches. For instance, the equations of the morph frequencies are reminiscent of those governing allele frequency change in classical population genetics models, except that in our approach the means and variances are not fixed. Similarly, the dynamics of the morph means are reminiscent of those of classical quantitative genetics, but we go one step further by deriving the dynamics of morph variances instead of assuming that they are fixed. In this way, our approach relaxes some key assumptions of classical population and quantitative genetics while providing a more dynamical perspective than classical invasion analyses.

Dynamics of Ecological Variables and Morph Frequencies

In this section, we derive the dynamics of the fast variables, which are the class densities $n^k(t)$ and class-specific morph frequencies $f_i^k(t)$. We also introduce the idea of weighting each class by its reproductive value in order to calculate the net effect of selection on the change of frequency of a given morph.

Dynamics of Densities

Collecting all the class densities $n^k(t)$ in a vector $\mathbf{n}$, we can write

$$\frac{d\mathbf{n}}{dt} = \bar{\mathbf{R}}\mathbf{n}, \tag{8}$$

where $\bar{\mathbf{R}}$ is the matrix of average vital rates $\bar{r}^{jk}$. Using equation (7), we have $\bar{r}^{jk} = \sum_i f_i^k r^{jk}(\bar{z}_i^k) + O(\varepsilon^2)$, so the dynamics of class densities depend, to the zeroth order, only on the morph frequencies and means. More explicitly, we have

$$\frac{dn^k}{dt} = \sum_j \sum_i r^{kj}(\bar{z}_i^j) f_i^j n^j + O(\varepsilon^2). \tag{9}$$

Similarly, the vector of class frequencies $\mathbf{f} = \mathbf{n}/n$ has the following dynamics (Lion 2018*a*):

$$\frac{d\mathbf{f}}{dt} = \bar{\mathbf{R}}\mathbf{f} - \bar{r}\mathbf{f}, \tag{10}$$

where $\bar{r} = \mathbf{1}^{\top}\bar{\mathbf{R}}\mathbf{f} = \sum_j \sum_k \bar{r}^{jk} f^k$ is the average growth rate of the total population. Again, expansion (7) shows that the dynamics of class frequencies is $O(1)$ and solely determined by the morph frequencies and morph means.

Dynamics of Morph Frequencies

In appendix A, we show that the dynamics of the within-class morph frequencies f_i^k can be written as

$$\begin{aligned}\frac{\mathrm{d}f_i^k}{\mathrm{d}t} &= \sum_j \frac{f^j}{f^k}\left(r_i^{kj} f_i^j - f_i^k \bar{r}^{kj}\right) \\ &= \sum_j \frac{f^j}{f^k}\left(r^{kj}(\bar{z}_i^j) f_i^j - f_i^k \sum_\ell f_\ell^j r^{kj}(\bar{z}_\ell^j)\right) + O(\varepsilon^2),\end{aligned} \tag{11}$$

which shows that the morph frequencies f_i^k also have fast dynamics that depend only on the morph positions and frequencies. Equation (11) is the class-structured extension of the first line of equation (17) in Sasaki and Dieckmann (2011) and is a class-structured version of the replicator equation (Crow and Kimura 1970; Ewens 2004).

Later, we shall see that it is also useful to introduce the total frequency of morph i, $f_i = \sum_k f_i^k f^k$, and the vector $\mathbf{u}_i$ collecting the morph frequencies $u_i^k = f_i^k f^k / f_i$, which gives the fraction of morph i individuals that are in class k. The dynamics of $\mathbf{u}_i$ is then

$$\frac{\mathrm{d}\mathbf{u}_i}{\mathrm{d}t} = \bar{\mathbf{R}}_i \mathbf{u}_i - \bar{r}_i \mathbf{u}_i, \tag{12}$$

where $\bar{\mathbf{R}}_i$ is the matrix of morph-specific average rates, $\bar{r}_i^{kj}$, and $\bar{r}_i = \mathbf{1}^{\top}\bar{\mathbf{R}}_i\mathbf{u}_i$ is the average growth rate of morph i. Hence, equation (12) is the morph-specific version of equation (10). Note the difference between the two morph frequencies f_i^k and u_i^k. The frequency f_i^k gives the fraction of morph i individuals among all class k individuals, while the frequency u_i^k is the fraction of class k individuals among all morph i individuals.

Dynamics of Morph Reproductive Values

As in Lion (2018*a*), equation (12) has a "companion" equation (or adjoint equation, in mathematical terms), which gives the dynamics of the vector of individual reproductive values for morph i, $\mathbf{v}_i$:

$$\frac{\mathrm{d}\mathbf{v}_i^{\top}}{\mathrm{d}t} = -\mathbf{v}_i^{\top}\bar{\mathbf{R}}_i + \bar{r}_i \mathbf{v}_i^{\top}. \tag{13}$$

The reproductive value $v_i^k(t)$ measures the relative contribution to the future of a morph i individual in class k at time t and therefore gives an instantaneous measure of the relative quality of class k from the point of view of morph i. Note that $\mathbf{v}_i$ and $\mathbf{u}_i$ are conormalized such that $\mathbf{v}_i^{\top}\mathbf{u}_i = 1$. This conormalization condition means that the average quality of a morph i individual is 1 at all times (Lion and Gandon 2021). Later in the article, we will show that we can weight individuals in different classes by their reproductive values in order to calculate the net effect of selection on morph i, which will allow us to reduce the dimension of the eco-evolutionary dynamics.

Dynamics of Morph Means and Variances

On the fast timescale where morph means and variances do not change much, equations (9) and (11) are sufficient to describe the eco-evolutionary dynamics of the population. We now look at the slower timescales corresponding to changes in the morph means $\bar{z}_i^k$ and morph variances V_i^k.

Dynamics of Morph Means

In appendix B, we show that the dynamics of morph means take the form of a class-structured Price equation (similar to those derived in Lion 2018*a*, 2018*b*). Using expansion (6) and assuming that the morph distributions are and remain symmetric, we obtain

$$\frac{\mathrm{d}\bar{z}_i^k}{\mathrm{d}t} = \sum_j \frac{u_i^j}{u_i^k}\left[(\bar{z}_i^j - \bar{z}_i^k) r^{kj}(\bar{z}_i^j) + V_i^j \left.\frac{\partial r^{kj}}{\partial z}\right|_{z=\bar{z}_i^j}\right] + O(\varepsilon^4). \tag{14}$$

The first term between brackets in equation (14) represents the effect of demographic transitions between classes and can be viewed as a migration term. In the absence of other processes, the phenotypic differentiation $\bar{z}_i^j - \bar{z}_i^k$ will tend to be consumed by demographic transitions from classes j to k, which occur at rates $r^{kj}(\bar{z}_i^k)$. However, selection itself can generate phenotypic differentiation. The second term between brackets in equation (14) corresponds to the effect of directional selection on morph i within class j and depends on the variance V_i^j of morph i in class j and on the marginal effect of the trait on the vital rates, evaluated at the morph mean in class j. Finally, the ratio u_i^j/u_i^k gives the relative abundance of classes j and k in the population of morph i individuals and is used as a weight to obtain the net change of the morph mean in class k, so that classes with a low frequency in the population do not contribute much. Note that in the absence of class structure, the first term between brackets vanishes and we recover equation (25) in Sasaki and Dieckmann (2011).

It may not be immediately obvious that $\bar{z}_i^k$ is a slow variable. Indeed, although V_i^j is $O(\varepsilon^2)$ by assumption, the first term between brackets is not necessarily small. For many biologically realistic applications, however, we can further

assume that the morph means in the different classes are not too different, and more precisely that the phenotypic differentiation $\bar{z}_i^j - \bar{z}_i^k$ is $O(\varepsilon)$, in which case the $\bar{z}_i^k$'s will change on a slower timescale compared with the morph frequencies f_i^k's and the class densities n^k. In a quasi-equilibrium approximation, this means that while the $\bar{z}_i^k$ change slowly, the fast variables immediately track this change so that the right-hand sides (RHSs) of equations (9)–(11), which all explicitly depend on the morph means $\bar{z}_i^k$, can be set to zero. More generally, we can use a perturbation expansion to show that the $\bar{z}_i^k$'s have a fast component (corresponding to the homogenization of morph means due to between-class demographic transitions) and a slow component (corresponding to the effect of selection), so that we can relax the assumption that the differentiations $\bar{z}_i^j - \bar{z}_i^k$ are initially small (sec. S3 of the supplemental PDF).

Dynamics of Morph Variances

A classical quantitative genetics approach would typically focus on equation (14) under the assumption of constant variances. However, this is not sufficient to understand how disruptive selection may shape multimorph trait distributions, and for this we need to turn to the dynamics of the morph variances.

In appendix B, we show that the dynamics of the class-specific morph variances can be written as

$$\begin{aligned}\frac{\mathrm{d}V_i^k}{\mathrm{d}t} = \sum_j \frac{u_i^j}{u_i^k}\Bigg[&(V_i^j - V_i^k + (\bar{z}_i^j - \bar{z}_i^k)^2) r^{kj}(\bar{z}_i^j) \\ &+ 2(\bar{z}_i^j - \bar{z}_i^k) V_i^j \frac{\partial r^{kj}}{\partial z}\bigg|_{z=\bar{z}_i^j} \\ &+ \frac{1}{2}(Q_i^j + (\bar{z}_i^j - \bar{z}_i^k)^2 V_i^j - V_i^j V_i^k) \frac{\partial^2 r^{kj}}{\partial z^2}\bigg|_{z=\bar{z}_i^j}\Bigg] \\ &+ O(\varepsilon^5).\end{aligned} \tag{15}$$

The term on the first line corresponds to the effect of demographic transitions between classes on variance. Basically it tells us that even in the absence of selection, changes in the morph variance in class k can be observed if the morph distributions are different across classes (e.g., if the morph mean and variance in class j differ from those in class k). The term on the second line represents the effect of directional selection on the morph variance in class k, which will be greater when there is substantial phenotypic differentiation between the focal class and the other classes. Finally, the term on the third line represents the effect of disruptive selection on the morph variance and depends on the means, variances, and fourth central moments of the morph distributions in class j, $Q_i^j = \int (\xi_i^j)^4 \phi_i^j(z,t)\,\mathrm{d}z$. Note that in the absence of class structure, the first two lines vanish and we recover equation (33) in Sasaki and Dieckmann (2011).

If we assume, as in the previous section, that $\bar{z}_i^j - \bar{z}_i^k$ is $O(\varepsilon)$, then the terms on the first, second, and third lines are respectively $O(\varepsilon^2)$, $O(\varepsilon^3)$, and $O(\varepsilon^4)$, and it is immediately clear that the morph variances change on a slow timescale compared with the morph densities and frequencies. A more general argument can be obtained using the perturbation expansion approach detailed in section S3 of the supplemental PDF, as for the dynamics of the means.

Moment Closure

As typical of moment methods, the dynamics of morph variances (15) depend on higher-order moments, notably the fourth central moments Q_i^j. Hence, we need to close the system using a suitable moment closure approximation. For unstructured populations, Sasaki and Dieckmann (2011) studied two moment closure approximations, namely, the Gaussian approximation and the house-of-cards approximation. In this article, we focus on the Gaussian approximation and therefore assume that the morph distributions $\phi_i^k(z)$ are normal. Biologically, this means that the total distribution of the trait can be viewed as a weighted sum of normal distributions. Mathematically, this entails that $Q_i^j = 3(V_i^j)^2$, which is sufficient to close the system. Importantly, the assumption of normal morph distributions matters only when calculating the dynamics of variances.

Adding Mutation

So far, we have analyzed the effect of selection on the dynamics of densities, morph frequencies, morph means, and variances, in the absence of mutation. There are several ways to incorporate mutation in our framework, but the simplest is to assume that mutation is independent of birth events and is unbiased at the morph level. With these assumptions, we show in appendix E that the only effect of mutation is to increase morph variance by a term V_M^k, which is the mutational variance in class k (which is the product of the mutation rate μ^k times the variance of the mutation kernel in class k). Thus, any depletion of morph variance due to stabilizing selection will tend to be regenerated by mutation.

Morph-Level Dynamics: Projection on Reproductive Value Space

The above analysis allows us to derive dynamical equations for the ecological densities, morph frequencies, morph means, and morph variances, but this results in a high-dimensional system. In this section, we show that

we can reduce the dimension of this system by tracking the moments of average morph distributions, where the average is obtained by weighting each class by both its quality and its quantity. There are several possible weightings, but the most convenient is to use reproductive values as weights, as this choice leads to simpler equations and ensures that we capture the net effect of selection on a given morph (Fisher 1930; Taylor 1990; Lehmann and Rousset 2014; Gardner 2015; Grafen 2015; Lion 2018*a*).

Reproductive Value–Weighted Trait Distributions

We use the reproductive values we introduced in the "Dynamics of Morph Reproductive Values" section to define a weighted trait distribution (Lion 2018*a*):

$$\tilde{\phi}_i(z,t) = \sum_k c_i^k(t)\phi_i^k(z,t), \tag{16}$$

where $c_i^k(t) = v_i^k(t)u_i^k(t)$ is the class reproductive value of morph i in class k at time t. Equation (16) weighs the class-specific morph distribution by both the quantity $u_i^k(t)$ and the quality $v_i^k(t)$ of class k individuals within the morph i subpopulation. As intuitively expected, the quality and quantity of a class may change over time, so these are dynamical variables (Lion 2018*a*; Lion and Gandon 2021). Figure 1 gives a graphical illustration of the process by which class- and morph-specific distributions can be aggregated to obtain morph-specific reproductive value–weighted distributions.

Biologically, equation (16) gives us an appropriate metric to measure the average effect, across all classes, of selection acting on a given morph. By accounting for the relative qualities of each class, it is possible to get rid of any spurious effect due to intrinsic demographic differences between classes (e.g., when one class has a systematically higher productivity than the others, irrespective of the individuals' genotypes). Any observed change in the reproductive value–weighted trait distribution will therefore be the result of selection only.

Projection on Reproductive Value Space

From a mathematical point of view, equation (16) corresponds to a projection onto a lower-dimensional space, on which we can approximate the dynamics of the moments of the class-specific morph distributions by the dynamics of the moments of the reproductive value–weighted morph distribution. For simplicity, we call this approximation the projection on reproductive value space. Mathematical details are given in appendix C, but the key biological insight is that if morph distributions are sufficiently clustered around the morph mean, the dynamics of the morph moments on the slow timescale will closely track the moments of the reproductive value–weighted morph distribution.

Equation (13) shows that the dynamics of the morph reproductive values are $O(1)$, so that reproductive values change on the same timescale as class frequencies. On this fast timescale, we can derive a quasi-equilibrium approximation from equations (10) and (13),

$$\bar{\mathbf{R}}_i\mathbf{u}_i = \mathbf{v}_i^{\mathsf{T}}\bar{\mathbf{R}}_i = \mathbf{0}, \tag{17}$$

so that the vectors of class frequencies and reproductive values are respectively the right and left eigenvectors of the matrix $\bar{\mathbf{R}}_i$ associated with eigenvalue 0, where it follows from equation (7) that $\bar{\mathbf{R}}_i$ has elements $\bar{r}_i^{kj} = r^{kj}(\bar{z}_i^j) + O(\varepsilon)$. This is a multimorph extension of a standard result from monomorphic theory (Taylor 1990; Rousset 2004; Lehmann and Rousset 2014; Lion 2018*a*, 2018*b*; Priklopil and Lehmann 2020).

Dynamics of Morph Means on Reproductive Value Space

On the slow timescale, the dynamics of the morph mean across all classes can be approximated, to leading order, by the dynamics of the reproductive-weighted morph mean (app. C)

$$\frac{\mathrm{d}\tilde{z}_i}{\mathrm{d}t} = \tilde{V}_i \sum_j \sum_k v_i^k \left.\frac{\partial r^{kj}}{\partial z}\right|_{z=\tilde{z}_i} u_i^j + O(\varepsilon^4), \tag{18}$$

where $\tilde{z}_i$ and $\tilde{V}_i$ are the mean and variance of $\tilde{\phi}_i(z,t)$. In matrix form, equation (18) can be written as

$$\frac{\mathrm{d}\tilde{z}_i}{\mathrm{d}t} = \tilde{V}_i\,\mathbf{v}_i^{\mathsf{T}}\mathbf{S}_i\mathbf{u}_i + O(\varepsilon^4), \tag{19}$$

where

$$\mathbf{S}_i = (\partial\mathbf{R}/\partial z)|_{z=\tilde{z}_i}$$

is the directional selection matrix.

The effect of selection on the morph mean is thus scaled by the morph variance, $\tilde{V}_i$, and the direction of selection is given by the selection gradient, $\mathbf{v}_i^{\mathsf{T}}\mathbf{S}_i\mathbf{u}_i$, which depends on (1) the marginal effect of a change in the trait on the between-class transition rates $r^{kj}(z)$, evaluated at the morph mean; (2) the relative quality of class k for morph i individuals, measured by the reproductive value v_i^k; and (3) the relative quantity u_i^k of class k individuals among morph i individuals. The class frequencies, morph frequencies, and reproductive values are all calculated using the zeroth-order terms of equations (8)–(11). In particular, the vectors $\mathbf{v}_i$ and $\mathbf{u}_i$ satisfy equation (17).

The selection gradient $\mathbf{v}_i^{\mathsf{T}}\mathbf{S}_i\mathbf{u}_i$ is the multimorph extension of the classical expression for the class-structured selection gradient of invasion analyses (Taylor 1990; Rousset 1999, 2004; Lehmann and Rousset 2014; Lion 2018*a*, 2018*b*; Priklopil and Lehmann 2020), which can be recovered by noting that in the single-morph case, $f_i^k = f_i = 1$, so that

$\mathbf{u}_i = \mathbf{f}$ and $\mathbf{v}_i = \mathbf{v}$. Equation (18) also has similarities with some quantitative genetics results (e.g., eq. [8] in Barfield et al. 2011), but with two subtle differences. First, equation (8) in Barfield et al. (2011) is derived under frequency independence, and as a result the directional selection matrix depends on the derivatives of the mean transition rates $\bar{r}^{kj}$ with respect to the mean trait, instead of the derivatives of the transition rates $r^{kj}(z)$ with respect to z (Iwasa et al. 1991; Day 2005; Lion 2018*c*). Second, equation (8) in Barfield et al. (2011) also depends on the class-specific means and is therefore unclosed (see app. C for further discussion).

Figure 2 illustrates the convergence to reproductive value space in a simple two-class model. The dynamics of the morph means in classes *A* and *B* (black lines) quickly relax then closely follow the prediction of equation (18) (gray line) until the eco-evolutionary dynamics stabilize.

Dynamics of Morph Variances on Reproductive Value Space

As for the morph mean, we can use reproductive values to derive an aggregate equation for the dynamics of the morph variances. In its most compact form, it takes the form of a Price equation (app. C):

$$\frac{\mathrm{d}\tilde{V}_i}{\mathrm{d}t} = \sum_j \sum_k v_i^k \underset{\phi_i^j}{\mathrm{Cov}}((z-\tilde{z}_i)^2, r^{kj}(z))u_i^j + \tilde{V}_{M,i}, \quad (20)$$

where the covariance is calculated over the distribution $\phi_i^j(z,t)$. The term $\tilde{V}_{M,i} = \sum_i c_i^k V_M^k$ is a reproductive value–weighted mutational variance.

The oligomorphic approximation (together with a Gaussian closure at the morph level) allows us to further expand the covariance (see app. C) as

$$\frac{\mathrm{d}\tilde{V}_i}{\mathrm{d}t} = 2(\tilde{V}_i)^2[\mathbf{v}_i^\top \mathbf{F}_i \mathbf{u}_i + \mathbf{v}_i^\top \mathbf{S}_i(\mathbf{d}_i \circ \mathbf{u}_i)] + \tilde{V}_{M,i} + O(\varepsilon^5), \quad (21)$$

where the notation $\circ$ denotes the elementwise (Hadamard) product. The first term between brackets depends on the matrix

$$\mathbf{F}_i = \frac{1}{2}\frac{\partial^2 \mathbf{R}}{\partial z^2}\bigg|_{z=\tilde{z}_i}.$$

It is the class-structured analog of equation (37) in Sasaki and Dieckmann (2011) and gives the net effect of the curvature of the fitness functions $r^{kj}(z)$ on the dynamics of variance.

The second term between brackets depends on the directional selection matrix $\mathbf{S}_i$ and on the vector $\mathbf{d}_i$ of phenotypic differentiations $(\bar{z}_i^j - \tilde{z}_i)/\tilde{V}_i$. The operation $\mathbf{d}_i \circ \mathbf{u}_i$ returns a vector with elements $u_i^j(\bar{z}_i^j - \tilde{z}_i)/\tilde{V}_i$ $(1 \le j \le K)$. This second term represents the additional effect of directional selection on the dynamics of morph variance. Intuitively, these two effects can be understood from the decomposition of the morph variance into class-specific morph moments:

$$\tilde{V}_i = \sum_k c_i^k V_i^k + \sum_k c_i^k[(\bar{z}_i^k)^2 - (\tilde{z}_i)^2].$$

The first term shows that when the class means are equal, the morph variance $\tilde{V}_i$ is the weighted average of the class-specific morph variances V_i^k. The second term shows that even when the class variances V_i^k are zero, substantial differentiation between classes $(\bar{z}_i^k \neq \tilde{z}_i)$ can contribute to morph variance. Hence, changes in the mean traits have a direct effect on the dynamics of the variance, which is proportional to the strength of selection in each class

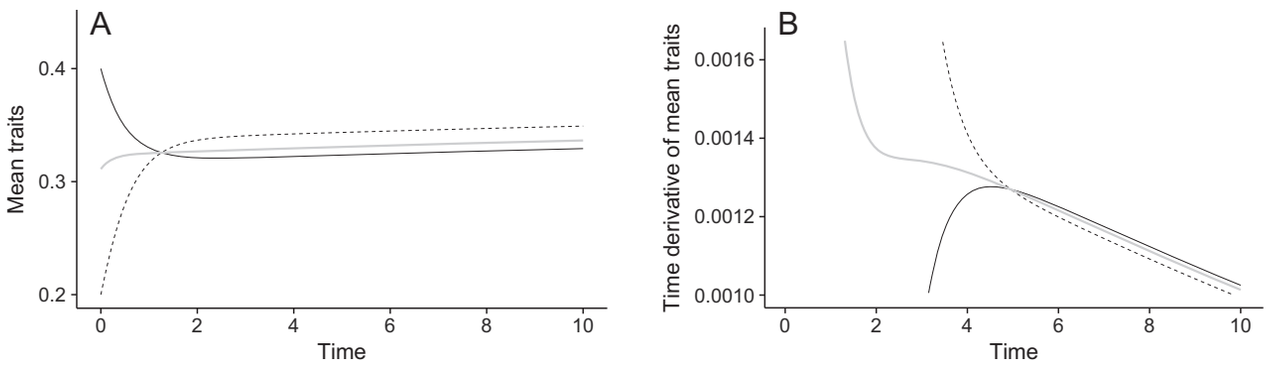

Figure 2: Illustration of the relaxation to reproductive value space in a two-class model. *A*, Convergence of the class-specific morph means $\bar{z}_1^A$ (black solid line) and $\bar{z}_1^B$ (dashed line) to the reproductive value–weighted mean $\tilde{z}_1$ (gray line). *B*, Convergence of the time derivatives $\mathrm{d}\bar{z}_{A,1}/\mathrm{d}t$ (black solid line) and $\mathrm{d}\bar{z}_{B,1}/\mathrm{d}t$ (dashed line), shown to converge toward the prediction of the right-hand side of equation (18) (gray line). The simulation is the same as in figure S3*B*, to which the reader is referred for additional details.

(captured by the matrix $\mathbf{S}_i$) and to the level of phenotypic differentiation in each class, compared with the mean morph value (captured by the vector $\mathbf{d}_i$).

Note that the second term between brackets in equation (21) still depends on the class-specific morph means, $\bar{z}_i^j$. However, as shown in Lion (2018*b*), the vector of phenotypic differentiation is a fast variable and can be approximated, on the reproductive value space, by a quasi-equilibrium expression that we can express solely in terms of $\mathbf{v}_i$, $\mathbf{u}_i$, $\bar{\mathbf{R}}(\bar{z}_i)$, and $\mathbf{S}_i$, leading to a closed system at the morph level (sec. S2 of the supplemental PDF; Lion 2018*b*). Although the resulting expression in the general case is not very enlightening, we show in the "Applications" section and appendix D that it yields very simple expressions when the model has only two classes.

Putting Everything Together

The above derivation yields a coupled system of differential equations describing how ecological densities, morph frequencies, morph means, and morph variances change over time. There are three main ways to use these equations, depending on whether the biological question of interest focuses on dynamics or statics.

Eco-Evolutionary Dynamics: Oligomorphic Approximation

The oligomorphic approximation allows us to derive an approximation of the full eco-evolutionary dynamics that takes the form of a fast-slow system with different intrinsic timescales. We collect these equations here, for ease of reference:

$$\frac{\mathrm{d}n^k}{\mathrm{d}t} = \sum_j \sum_i r^{kj}(\bar{z}_i^j) f_i^j n^j, \tag{22a}$$

$$\frac{\mathrm{d}f_i^k}{\mathrm{d}t} = \sum_j \frac{f_i^j}{f^k}\left(r^{kj}(\bar{z}_i^j) f_i^j - f_i^k \sum_\ell f_\ell^j r^{kj}(\bar{z}_\ell^j)\right), \tag{22b}$$

$$\frac{\mathrm{d}\bar{z}_i^k}{\mathrm{d}t} = \sum_j \frac{u_i^j}{u_i^k}\left[(\bar{z}_i^j - \bar{z}_i^k) r^{kj}(\bar{z}_i^j) + V_i^j \left.\frac{\partial r^{kj}}{\partial z}\right|_{z=\bar{z}_i^j}\right], \tag{22c}$$

$$\begin{aligned}\frac{\mathrm{d}V_i^k}{\mathrm{d}t} = \sum_j \frac{u_i^j}{u_i^k}\Bigg[&(V_i^j - V_i^k + (\bar{z}_i^j - \bar{z}_i^k)^2) r^{kj}(\bar{z}_i^j) \\ &+ 2(\bar{z}_i^j - \bar{z}_i^k) V_i^j \left.\frac{\partial r^{kj}}{\partial z}\right|_{z=\bar{z}_i^j} \\ &+ \frac{1}{2}(3(V_i^j)^2 + (\bar{z}_i^j - \bar{z}_i^k)^2 V_i^j - V_i^j V_i^k) \\ &\times \left.\frac{\partial^2 r^{kj}}{\partial z^2}\right|_{z=\bar{z}_i^j}\Bigg] + V_M^k.\end{aligned} \tag{22d}$$

Here, we have used the Gaussian moment closure and dropped the order terms for simplicity. This system can be numerically integrated and allows us to track the joint dynamics of ecological and evolutionary variables. It also provides analytical insights into the observed dynamics. Thus, equations (22) can be viewed as an extension of classical quantitative genetics methods to take into account ecological feedbacks, class structure, multimodal distributions and the dynamics of variance. The accuracy of the approximation will tend to decrease as within-morph variation or mutation becomes too large.

Eco-Evolutionary Dynamics: Projection on Reproductive Value Space

The projection on reproductive value space can be used to reduce the dimension of our system and derive the dynamics of the morph means and variances:

$$\frac{\mathrm{d}\tilde{z}_i}{\mathrm{d}t} = \tilde{V}_i \mathbf{v}_i^\top \mathbf{S}_i \mathbf{u}_i, \tag{23a}$$

$$\frac{\mathrm{d}\tilde{V}}{\mathrm{d}t_i} = 2(\tilde{V}_i)^2 [\mathbf{v}_i^\top \mathbf{F}_i \mathbf{u}_i + \mathbf{v}_i^\top \mathbf{S}_i (\mathbf{d}_i \circ \mathbf{u}_i)] + \tilde{V}_{M,i}, \tag{23b}$$

where $\mathbf{d}_i$ measures the phenotypic differentiation between classes. Both $\tilde{z}_i$ and $\tilde{V}_i$ are slow variables when the morph variances are small. We can then use a quasi-equilibrium approximation, as typically done when dealing with fast-slow systems. In particular, the frequencies $\mathbf{u}_i$ and reproductive values $\mathbf{v}_i$ satisfy the following quasi-equilibrium relationships:

$$\mathbf{0} = \mathbf{R}(\tilde{z}_i)\mathbf{u}_i = \mathbf{v}_i^\top \mathbf{R}(\tilde{z}_i). \tag{24}$$

Note that in these equations the matrices $\mathbf{R}$, $\mathbf{S}_i$, and $\mathbf{F}_i$ depend on the ecological densities and morph frequencies (see, e.g., examples 2 and 3 below), which can be calculated from

$$\frac{\mathrm{d}n^k}{\mathrm{d}t} = \sum_j \sum_i r^{kj}(\tilde{z}_i) f_i^j n^j, \tag{25a}$$

$$\frac{\mathrm{d}f_i^k}{\mathrm{d}t} = \sum_j \frac{f_i^j}{f^k}\left(r^{kj}(\tilde{z}_i) f_i^j - f_i^k \sum_\ell f_\ell^j r^{kj}(\tilde{z}_\ell)\right). \tag{25b}$$

These are simply equations (22a) and (22b) where the class means $\bar{z}_i^j$ have been replaced by the morph means $\tilde{z}_i$. As the morph means $\tilde{z}_i$ change slowly, the fast variables n^k and f_i^k will quickly track these changes. In practice, either we can calculate, for a given value of $\tilde{z}_i$, the quasi-equilibrium values of n^k and f_i^k by setting the RHSs of equations (25) to zero or we can numerically integrate equations (25), together with equations (23), to obtain the values of n^k and f_i^k at any given time.

Eco-Evolutionary Statics

Although our framework is geared toward dynamics, it is interesting to show how we can use equations (23) to derive analytical information on the potential eco-evolutionary end points and their stability and therefore recover results from invasion analyses. We then use a step-by-step analysis. First, we assume that morph means and variances change so slowly that the ecological dynamics reach an equilibrium attractor. We then plug this information into the dynamics of morph means and calculate evolutionary singularities from

$$\hat{\mathbf{v}}_i^{\top}\hat{\mathbf{S}}_i\hat{\mathbf{u}}_i = 0,$$

where the hat indicates that all of these quantities are calculated on the ecological attractor. This is basically the same result as we could obtain with a traditional invasion analysis (see, e.g., Taylor 1990; Rousset 2004; Priklopil and Lehmann 2020) but in a polymorphic resident population. As shown by Sasaki and Dieckmann (2011), we can use the dynamics of the means near these singularities to investigate their convergence stability (i.e., whether or not they attract the trait dynamics). Similarly, we can investigate the evolutionarily stability of these singularities (i.e., whether selection is disruptive or stabilizing) by evaluating the dynamics of variance near these singularities. As shown by Sasaki and Dieckmann (2011), the singularities z_i^* are all evolutionarily stable if and only if the morph variances converge to zero, leading to the conditions

$$\hat{\mathbf{v}}_i^{\top}\hat{\mathbf{F}}_i\hat{\mathbf{u}}_i + \hat{\mathbf{v}}_i^{\top}\hat{\mathbf{S}}_i(\hat{\mathbf{d}}_i \circ \hat{\mathbf{u}}_i) < 0$$

when $\tilde{z}_i = z_i^*$. The first term was previously obtained using invasion analyses (see, e.g., the first term of eq. [34A] in Ohtsuki et al. 2020). The second term captures how directional selection in the different classes contributes to disruptive selection and probably bears some resemblance with the first term of equation (34B) in Ohtsuki et al. (2020), although a precise comparison of the two results is currently beyond our reach.

Applications

As proof-of-concept examples, we apply our general framework to two-habitat migration-selection models. We start by giving general dynamical equations for these models and then explore three different biological scenarios that illustrate various aspects of our framework. From now on, we deliberately simplify the mathematical expressions by omitting the order terms and using the more intuitive notations $\bar{z}_i$ and V_i to denote the (reproductive value–weighted) morph means and variances instead of the tilded versions.

General Results for Two-Habitat Migration-Selection Models

We consider a population inhabiting two habitats, A and B, coupled by migration. We define m_{jk} as the migration rate from k to j and $\rho_k(z)$ as the growth rate of individuals in habitat k, which is a function of a focal trait z. With our notations, we have

$$\begin{aligned} r^{AA}(z) &= \rho_A(z) - m_{BA}, \\ r^{AB}(z) &= m_{AB}, \\ r^{BA}(z) &= m_{BA}, \\ r^{BB}(z) &= \rho_B(z) - m_{AB}. \end{aligned}$$

Because the migration rates do not depend on the focal trait z, the dynamics of morph means and variances take a simple form using the projection on reproductive value space (app. D),

$$\frac{\mathrm{d}\bar{z}_i}{\mathrm{d}t} = V_i[c_i^A\rho_A'(\bar{z}_i) + c_i^B\rho_B'(\bar{z}_i)], \tag{26a}$$

$$\begin{aligned} \frac{\mathrm{d}V_i}{\mathrm{d}t} = (V_i)^2 \Bigg[& c_i^A\rho_A''(\bar{z}_i) + c_i^B\rho_B''(\bar{z}_i) \\ & + 2\frac{(c_i^A c_i^B)^{3/2}}{\sqrt{m_{AB}m_{BA}}}(\rho_B'(\bar{z}_i) - \rho_A'(\bar{z}_i))^2 \Bigg] \\ & + c_i^A V_M^A + c_i^B V_M^B, \end{aligned} \tag{26b}$$

together with the following quasi-equilibrium expressions for the class reproductive values (app. D; sec. S4 of the supplemental PDF):

$$c_i^B = v_i^B u_i^B = \frac{m_{AB}(u_i^B)^2}{m_{BA}(u_i^A)^2 + m_{AB}(u_i^B)^2} = 1 - c_i^A. \tag{27}$$

In practice, the dynamics of the densities and morph frequencies can be obtained from

$$\frac{\mathrm{d}n^k}{\mathrm{d}t} = \sum_j \sum_i r^{kj}(\bar{z}_i) f_i^j n^j, \tag{28a}$$

$$\frac{\mathrm{d}f_i^k}{\mathrm{d}t} = \sum_j \frac{f^j}{f^k}\left(r^{kj}(\bar{z}_i) f_i^j - f_i^k \sum_\ell f_\ell^j r^{kj}(\bar{z}_\ell) \right), \tag{28b}$$

which are simply equations (25).

Example 1: Local Adaptation under Mutation-Selection-Migration Balance

In our first example, we revisit a classic model of local adaptation and investigate how migration and selection interplay to favor or hamper the generation of polymorphism in a population that can exploit two habitats with different qualities. In contrast with previous studies, we

provide dynamical equations that capture the notion of habitat quality in polymorphic populations through the concept of morph-specific reproductive values we introduced in the previous sections.

We assume that within each habitat reproduction depends on a trait z. We further assume that there is a quadratic cost to fecundity and that each habitat is characterized by a value θ_k, which minimizes the cost and which we call the habitat optimum. We thus write

$$\rho_k(z) = b - g(z - \theta_k)^2 - n^k,$$

where b is the birth rate, g is the fecundity cost, and θ_k is the optimum in habitat k. The same fitness functions were used in previous studies (Meszéna et al. 1997; Ronce and Kirkpatrick 2001; Débarre et al. 2013; Mirrahimi and Gandon 2020), but in contrast with most of these previous studies, we consider the possibility of asymmetric migration rates ($m_{AB} \neq m_{BA}$).

Together with equations (23), these expressions for the vital rates allow us to derive the following equations for the dynamics of morph means and variances (sec. S6 of the supplemental PDF):

$$\frac{\mathrm{d}\bar{z}_i}{\mathrm{d}t} = -2gV_i[\bar{z}_i - c_i^A\theta_A - c_i^B\theta_B], \tag{29}$$

$$\frac{\mathrm{d}V_i}{\mathrm{d}t} = -2gV_i^2\left[1 - \frac{4g}{m}(c_i^A c_i^B)^{3/2}(\theta_B - \theta_A)^2\right] + c_i^A V_M^A + c_i^B V_M^B, \tag{30}$$

where $m = \sqrt{m_{AB}m_{BA}}$ is the geometric mean of the dispersal rates, V_M^k are the habitat-specific mutational variances (app. E), and the morph-specific class reproductive values are given by their quasi-equilibrium expressions (eq. [27]). Using these equations, we investigate three main questions. First, what are the attractors of the eco-evolutionary dynamics? Second, when does selection lead to a unimodal versus bimodal equilibrium distribution? And third, what is the effect of habitat-specific mutation on the evolutionary outcome? Since a full analysis of the model would be beyond the reach of this article, we focus on the most salient features in the main text and briefly consider additional technicalities in section S6 of the supplemental PDF.

Evolutionary Attractors. From equation (29), we see that the morph means stabilize when

$$\bar{z}_i = c_i^A\theta_A + c_i^B\theta_B. \tag{31}$$

It is important to note that because of the quasi-equilibrium approximation, the class reproductive values are also functions of $\bar{z}_i$, so that equation (31) is only implicit. Nonetheless, the biological implication is that the potential attractors for the dynamics of the morph means correspond to the reproductive value–weighted mean of the habitat optima. Hence, the outcome of selection for a given morph depends on the relative difference in quality between habitats, measured by $c_i^B - c_i^A$. When $c_i^B > c_i^A$, the morph mean will be biased toward the optimum of habitat B, whereas the opposite will be observed for $c_i^B < c_i^A$. If both habitats have similar quality ($c_i^A = c_i^B = 1/2$), the morph mean will converge toward $(\theta_A + \theta_B)/2$. In the following, we fix $\theta_A = 0 = 1 - \theta_B$ without loss of generality.

Our analysis allows us to recover the important result that when the mean migration rate is sufficiently high, the eco-evolutionary dynamics settle on a unimodal distribution, while bimodal distributions can be generated if the mean migration rate is below a threshold m_c (fig. 3*A*; see also Débarre et al. 2013; Mirrahimi and Gandon 2020). Simulations of the full model without the oligomorphic approximation show that both the unimodal and the bimodal end points are accurately predicted by the projection on reproductive value space (fig. 3*A*).

At a unimodal distribution, the class reproductive values of the different morphs are equal (e.g., $c_1^B = c_2^B = c$ if we start with two morphs), so there is effectively a single morph in the population with mean trait value $\bar{z} = c$ (fig. 3*C*). In contrast, if different morphs have distinct class reproductive values (e.g., $c_1^B \neq c_2^B$), the eco-evolutionary dynamics converge toward a bimodal equilibrium distribution, where the morphs have different means ($\bar{z}_1 = c_1^B$ for morph 1 and $\bar{z}_2 = c_2^B$ for morph 2) and occur with different frequencies in the two habitats. The trait distributions in each habitat therefore have two peaks, one around $\bar{z}_1$ and one around $\bar{z}_2$, with the heights of the peaks being determined by the morph frequencies f_i^k and the densities n_A and n_B (fig. 3*B*). In section S6 of the supplemental PDF, we show how the positions $\bar{z}_1$ and $\bar{z}_2$ of each morph at equilibrium can be analytically calculated, thereby allowing us to recover previous results on local adaptation (Débarre et al. 2013; Mirrahimi and Gandon 2020).

Disruptive Selection and the Balance in Habitat Quality. When does the interplay between migration and selection leads to unimodal versus bimodal equilibrium trait distributions? To answer this question, we turn to the dynamics of morph variances (eq. [30]), which provides a useful interpretation of evolutionarily stability in terms of reproductive values. Indeed, the product $c_i^A c_i^B$ is a measure of the balance in habitat quality: it reaches its maximal value, $1/4$, when the habitats have equal qualities ($c_i^A = c_i^B = 1/2$) and is zero when $c_i^B = 0$ or $c_i^B = 1$. Selection on morph i is therefore stabilizing if the balance in habitat quality is below a

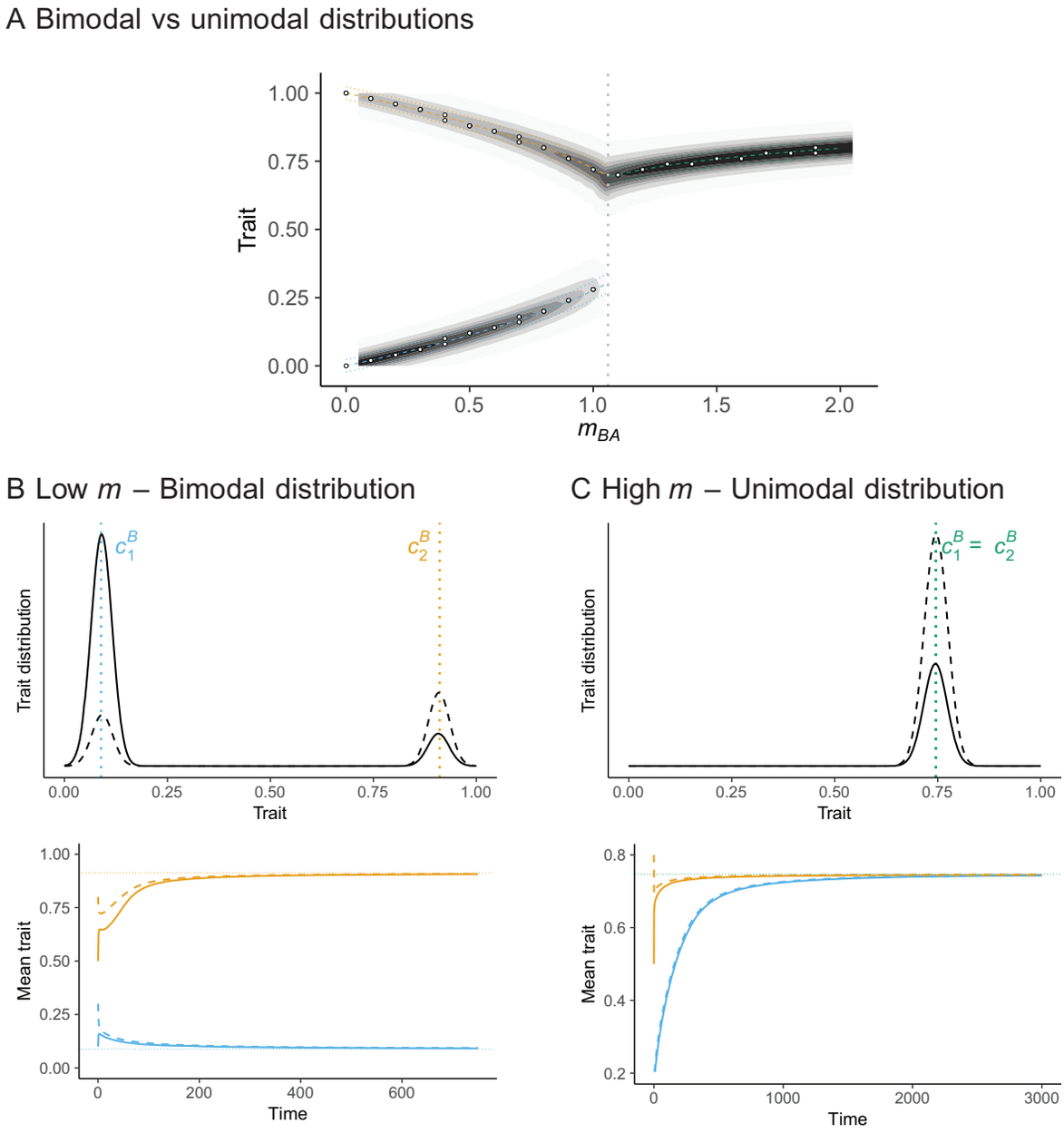

Figure 3: Bimodal versus unimodal equilibrium distributions (example 1). *A* shows how the equilibrium distribution changes when $m_{AB} = 0.8$ is fixed and m_{BA} varies. For simplicity, we show only the dimorphic solution in the bistability region. The vertical dotted line represents the value $m_{BA} \approx 1.06$, at which the dimorphic equilibrium loses its demographic stability and one of the two morphs becomes extinct. The analytical predictions using the projection on reproductive value space are also shown for the mean (dashed lines) ± standard deviation (dotted lines). The white circles show the results of numerical simulations of the full model, without the oligomorphic approximation. *B* and *C* show the equilibrium trait distributions and dynamics of mean traits in habitats *A* (solid line) and *B* (dashed line) obtained by numerical integration of a two-morph oligomorphic approximation for $m_{BA} = 0.4$ (*B*) or $m_{BA} = 1.4$ (*C*). The dotted lines indicate the value of the class reproductive value of habitat *B* for morphs 1 (blue) and 2 (orange), computed from the oligomorphic approximation. Parameter values: $b = 1$, $g = 2$, $m_{AB} = 0.8$, $V_M = 10^{-6}$.

threshold determined by the ratio between migration (m) and selection (g):

$$4\,c_i^A c_i^B < \left(\frac{2m}{g}\right)^{2/3}. \tag{32}$$

Note that for $m > g/2$ this is always satisfied, but with a lower mean migration rate, stability depends on the magnitude of habitat differentiation. Hence, for a fixed $m < g/2$, disruptive selection is possible and may lead to the splitting of an initially unimodal distribution into two peaks, provided the habitat qualities at the monomorphic evolutionary attractor are sufficiently similar ($c_i^A c_i^B$ large enough). Calculating $c_i^A c_i^B$ at the dimorphic attractor then shows that it is evolutionarily stable when $m < g/2$ and unstable otherwise. However, we note for completeness that there is a critical value $m_c < g/2$ above which the bimodal equilibrium loses its demographic stability and one of the two morphs becomes extinct (fig. S5*A*). Hence, for $m > m_c$, the only possible evolutionary outcome is a unimodal distribution. For $m < m_c$, multistability is possible, where the system can converge toward unimodal or bimodal distributions depending on initial conditions (sec. S6 of the supplemental PDF; Débarre et al. 2013).

Mutation-Selection-Migration Balance. With mutation and stabilizing selection, the morph variances can settle at a mutation-selection equilibrium. From equation (30), the equilibrium variance is then given by

$$V_i^* = \sqrt{\frac{c_i^A V_M^A + c_i^B V_M^B}{2g\left[1 - (4g/m)(c_i^A c_i^B)^{3/2}\right]}}. \tag{33}$$

The numerator is the effect of mutation on variance, which takes the form of a reproductive value–weighted average mutational variance, while the denominator gives the effect of selection. When only one habitat is present (e.g., $c_i^A = 1$ and $c_i^B = 0$), the morph variance at equilibrium is $\sqrt{V_M^A/2g}$, which is equation (17) in Débarre et al. (2013). For the bimodal attractor, both morphs have the same equilibrium variance if the mutational variance is the same in both habitats:

$$V_1^* = V_2^* = \sqrt{\frac{V_M}{2g(1 - (4m^2/g^2))}}. \tag{34}$$

On the other hand, if $V_M^A/V_M^B \neq 1$, each morph has a different equilibrium variance, which can be analytically calculated (sec. S6 of the supplemental PDF). Figure 4*A* shows that this accurately predicts the equilibrium values of morph variances under mutation-selection balance.

As mutation increases, the accuracy of the oligomorphic approximation is expected to decrease, as high mutation will tend to generate broader morph distributions. Nonetheless, figure 4*B* shows that our analytical prediction of the differentiation $D = \bar{z}^B - \bar{z}^A$ remains good even for relatively large values of the mutation variance (see sec. S6 of the supplemental PDF for a more detailed discussion). The approximation breaks down roughly when the mutation variance is of the same order as the morph variances.

Example 2: Evolution of Intraspecific Competition

In our second example, we assume that within each habitat competition between individuals depends on the competitive ability z. As previously, we further assume that there is a quadratic cost to competitiveness and that each habitat is characterized by a value, θ_k, that minimizes the cost. We thus write

$$\rho_k(z) = b - g(z - \theta_k)^2 - n^k \int a(z - y)\phi^k(y)\,\mathrm{d}y,$$

where the competition kernel $a(z - y)$ represents the effect of competition by an individual with trait y on an individual with trait z. Importantly, the fitness functions ρ_k now depend on the distributions $\phi^k(y, t)$, in contrast to our example 1. Following Sasaki and Dieckmann (2011), we decompose this distribution into a sum of the distributions $\phi_\ell(y, t)$, and for each of these distributions we use a Taylor expansion of the competition kernel near $y = \bar{z}_\ell^k$ to express the competition experienced by a focal individual in terms of the means of all of the other morphs. We obtain (sec. S7 of the supplemental PDF)

$$\rho_A(z) = b - g(z - \theta_A)^2 - n^A \sum_\ell f_\ell^A a(z - \bar{z}_\ell^A) + O(\varepsilon^2)$$

and a similar expression for the growth rate in habitat B. We can use these expressions to calculate the quantities $r^{kj}(\bar{z}_i)$ as well as the partial derivatives evaluated at $z = \bar{z}_i$ and plug these expressions in equations (22) to obtain the final approximation for this model (sec. S7 of the supplemental PDF).

This example is a perfect illustration of how all of the equations of system (22) are coupled. In particular, we have

$$\left.\frac{\partial r^{AA}}{\partial z}\right|_{z=\bar{z}_i} = -2g(\bar{z}_i - \theta_A) - n^A \sum_\ell f_\ell^A a'(\bar{z}_i^A - \bar{z}_\ell^A),$$

which shows that the competition experienced by morph i depends on the other morphs through their frequencies f_ℓ^A and mean trait values $\bar{z}_\ell^A$. Hence, the dynamics of the mean of morph i depends on the frequencies and mean traits of the other morphs.

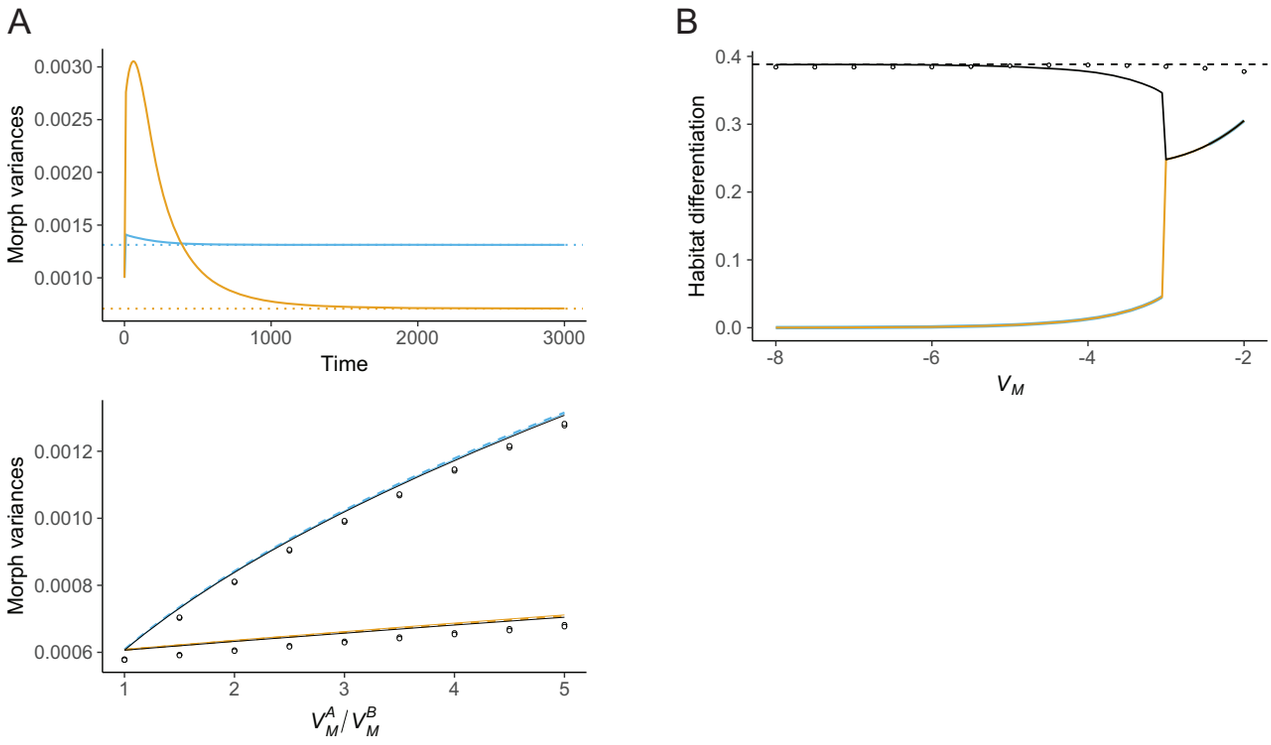

Figure 4: Effect of mutation (example 1). *A*, Effect of habitat-specific mutation. The top panel shows the dynamics of the variances of morphs 1 (blue) and 2 (orange), which converge to mutation-selection equilibrium values and are accurately predicted by the reproductive value–weighted formula (33) (dotted lines) with $V_M^A = 5 \times 10^{-6}$ and $V_M^B = 10^{-6}$. The bottom panel shows the effect of the ratio V_M^A/V_M^B on the variances V_i^A (solid line) and V_i^B (dashed line) for morphs 1 (blue) and 2 (orange). The white circles give the results of simulations of the full model without the oligomorphic approximation. *B*, Effect of the magnitude of mutational variance on the mean habitat differentiation $D = \bar{z}^B - \bar{z}^A$ at equilibrium (black line). Here, we use $V_M = V_M^A = V_M^B$. The dashed line gives the analytical prediction of equation (S44), the white circles the simulations results, the blue and orange lines the morph-specific habitat differentiation $\bar{z}_i^B - \bar{z}_i^A$. Parameters in all panels: $b = 1$, $g = 2$, $m_{AB} = 0.8$, $m_{BA} = 0.4$.

A full analysis of the model is beyond the scope of this article, but we show in figure 5 the dynamics for a specific choice of parameters. Figure 5*C* shows that starting from an effectively monomorphic population (where the two morphs have approximately the same mean values), disruptive selection leads to the splitting of the population into a bimodal distribution after $t \approx 1{,}000$. Disruptive selection is indicated by the explosion of morph variances at the same time (fig. 5*D*). The population then stabilizes around a dimorphic equilibrium distribution with means $\bar{z}_1^*$ and $\bar{z}_2^*$. Stabilizing selection is indicated by the decrease in variance after branching. Figure 5*B* further shows that the morphs have different frequencies in each habitat (i.e., morph 1 is slightly more abundant in habitat *B*, while morph 2 is slightly more abundant in habitat *A*), although they have similar values for the means and variances in both habitats.

This latter observation suggests that it may be interesting to find a simplified description of the population at the morph level by aggregating habitat-specific morph moments into a single measure. This is precisely the goal of the reproductive value projection, and we show in section S7 of the supplemental PDF that we obtain the following expression for the dynamics of morph means:

$$\frac{d\bar{z}_i}{dt} = V_i\left[-2g(\bar{z}_i - (c_i^A\theta_A + c_i^B\theta_B)) - \sum_j e_j a'(\bar{z}_j - \bar{z}_i)\right], \tag{35}$$

where e_j measures the average net fitness effect on individuals of morph j due to competition with the other morph. For morph 1, we have $e_1 = n_2^A c_1^A + n_2^B c_1^B$, and the expression for e_2 is obtained by swapping 1 and 2 subscripts. This expression shows that the class reproductive values give the proper weights to measure the intensity of competition in each habitat. Figure 5 shows that the reproductive value projection (dotted lines) accurately predicts both the trajectories and the end points of the densities, morph frequencies, morph means, and morph variances.

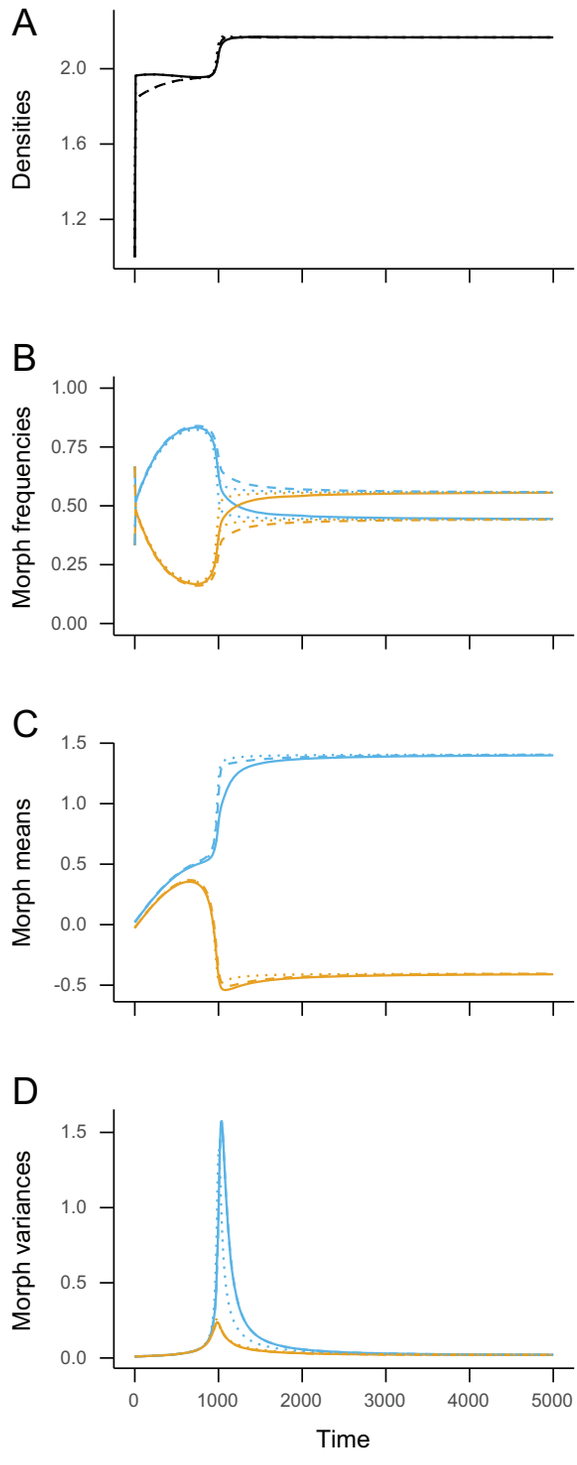

Figure 5: Eco-evolutionary dynamics of the resource competition model (example 2). *A*, Dynamics of densities of individuals n^k in habitats *A* (solid line) and *B* (dashed line). *B*, Dynamics of the morph frequencies f_i^k in habitats *A* (solid line) and *B* (dashed lines) for morphs 1 (blue) and 2 (orange). *C*, Dynamics of the morph means $\bar{z}_i^A$ (solid lines) and $\bar{z}_i^B$ (dashed lines). *D*, Dynamics of the morph variances V_i^A (solid lines) and V_i^B (dashed lines). In all panels, the results of a numerical integration of equations (22) are shown, and the corresponding predictions of the reproductive value projection (26)–(28) are overlaid as dotted lines. Parameters: $b = 1$, $g = 0.1$, $\theta_A = 0 = 1 - \theta_B$, $m_{AB} = m_{BA} = 0.3$, $a(x) = 0.5\exp(-x^2/8)$, $V_M = 10^{-5}$.

Equation (35) tells us that starting from a quasi-monomorphic situation (i.e. $\bar{z}_1 \approx \bar{z}_2$, so that $a'(\bar{z}_j - \bar{z}_i) \approx 0$), the population will converge toward the reproductive value–weighted mean of the habitat optima, $\bar{z}_i = c_i^A\theta_A + c_i^B\theta_B$. However, at this point selection becomes disruptive and a bimodal equilibrium distribution is eventually reached, with peaks located at the equilibrium morph means. From equation (35), the morph means satisfy

$$\bar{z}_1^* = c_1^A\theta_A + c_1^B\theta_B - \frac{e_1}{2g}a'(\bar{z}_1^* - \bar{z}_2^*),$$

$$\bar{z}_2^* = c_2^A\theta_A + c_2^B\theta_B + \frac{e_2}{2g}a'(\bar{z}_1^* - \bar{z}_2^*),$$

This provides an intuitive interpretation of the position of the two peaks of the equilibrium distribution as the deviation from the morph-specific mean habitat optimum due to competition with the other morph. In the single-class case, we recover the results of Kisdi (1999; see, e.g., her eq. [10]).

Example 3: Transient Out-of-Equilibrium Evolution in a Resource-Consumer Model

In our final example, we show how our approach can be used to analyze eco-evolutionary dynamics across different timescales. We consider a resource-consumer model where the resource is produced at different rates in the two habitats, so that $S^k(t)$ is the density of resource in habitat k at time t. We focus on the evolution of a consumer's exploitation rate, z, and assume a type II functional response such that

$$\rho_k(z) = b(z)\frac{S^k}{1 + \tau S^k} - d(z) - n^k, \tag{36}$$

where $b(z)$ is the fecundity rate, $d(z)$ is the mortality rate, and τ depends on the handling time. The dynamics of the resources S^A and S^B are given in section S8 of the supplemental PDF. In our thought experiment, we introduce the same low density of consumers in each habitat, but the genetic composition of each subpopulation is different: the initial distribution in each habitat is bimodal, with two peaks representing more prudent versus more rapacious consumers, but habitat *A* is predominantly seeded with more prudent consumers, while habitat *B* is predominantly seeded with more rapacious consumers (fig. 6*A*). Hence, the mean value of the trait in habitat *A* is initially lower than that in habitat *B*.

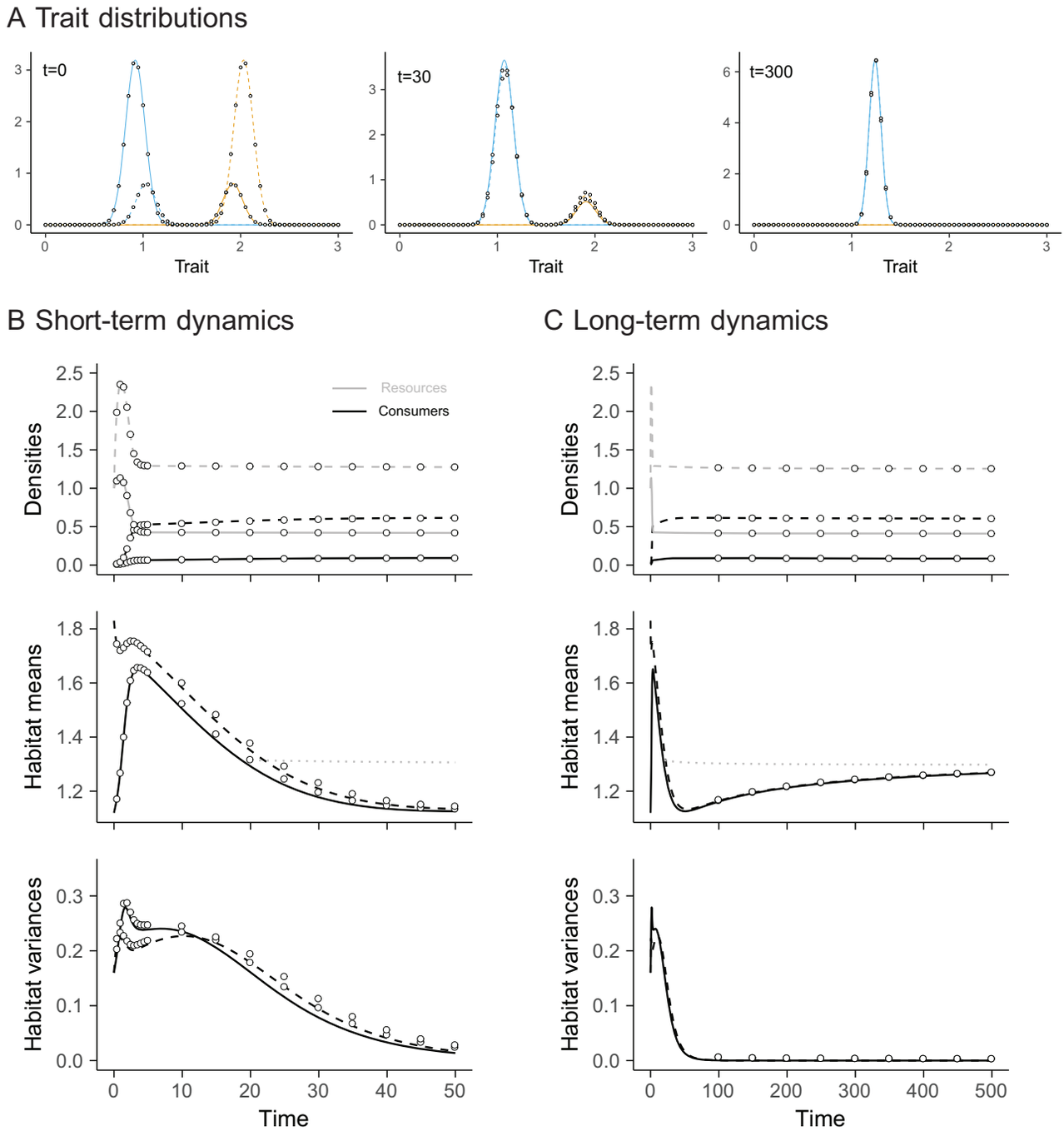

Figure 6: Eco-evolutionary dynamics of the resource-consumer model (example 3). *A* gives the distributions in each habitat at different times (plain line = habitat *A*, dashed line = habitat *B*, blue = morph 1, orange = morph 2). *B* and *C* give the dynamics of densities n^A and n^B (the consumer, black) and resources S^A and S^B (gray), habitat means $\bar{z}^A$ and $\bar{z}^B$, and habitat variances (plain line = habitat *A*, dashed line = habitat *B*). *B* and *C* show the same simulation results but on different timescales ($t = 50$ in *B*, $t = 500$ in *C*). In all panels, the main results are obtained using the reproductive value projection, and the circles show the results of the numerical simulations of the full model without the oligomorphic approximation. The horizontal dotted gray line is the prediction of the evolutionarily stable strategy $\bar{z}^A_{\text{eq}}$ (eq. [39]). Parameter values are given in section S8 of the supplemental PDF.

Our aim is to track how the habitat-specific means $\bar{z}^A$ and $\bar{z}^B$ change over time, much like a field quantitative geneticist would measure time series for phenotypes at different locations. In terms of the morph frequencies and morph means, we have $\bar{z}^k = \sum_i f_i^k \bar{z}_i^k$, and together with our projection on reproductive value space, this allows us to derive the following equation (sec. S8 of the supplemental PDF):

$$\frac{\mathrm{d}\bar{z}^A}{\mathrm{d}t} = (\bar{z}_1 - \bar{z}_2)\left[f_1^A(1 - f_1^A)\Delta\rho_A + \frac{f^B}{f^A} m_{AB}(f_1^B - f_1^A)\right] + \sum_i f_i^A V_i [c_i^A \rho_A'(\bar{z}_i) + c_i^B \rho_B'(\bar{z}_i)] \tag{37}$$

where $\Delta\rho_A = \rho_A(\bar{z}_1) - \rho_A(\bar{z}_2)$ is the average difference in growth rates between the two morphs.

Equation (37) is particularly enlightening about how the different timescales of eco-evolutionary dynamics interplay. The first line of equation (37) represents the contribution of the dynamics of frequencies to the change in the habitat-specific mean (i.e., what happens when the heights of the peaks change), while the second line represents the contribution of the change in morph means (i.e., when the position of the peaks change). When the distance between the two morphs $\bar{z}_1 - \bar{z}_2$ is large compared with the within-morph variances V_i, the dynamics of the mean trait in habitat A is dominated by the change in frequencies. The first term between brackets is reminiscent of classical population genetics equations and tells us that the dynamics of the mean trait in habitat A depends on the difference in growth rates between the two morphs, scaled by the variance $f_1^A(1 - f_1^A)$. The second term between brackets captures the effect of migration from B to A and reveals that $\bar{z}^A$ will tend to increase due to migration if the morph with the larger trait value is more abundant in habitat B. Thus, the first line in equation (37) captures the interplay between selection and migration typical of classical population genetics (or two-species ecological) models, but in contrast with these approaches it does not assume that there is no standing variation within a morph.

On the other hand, when the morph means are close ($\bar{z}_2 - \bar{z}_1$ is small, so that the population can be thought of as quasi monomorphic), the dynamics of the habitat mean is dominated by the change in morph means, which is described by the second line of equation (37). The term between brackets is now reminiscent of classical expressions for the selection gradient in class-structured populations, and the contribution of each morph now depends on the slopes of the morph's growth rates in each habitat.

Hence, if morph 1 has a higher growth rate but a lower slope than morph 2, it can be transiently selected in our model. In figure 6, we show that starting with an asymmetric bimodal distribution at time $t = 0$ (fig. 6*A*), the model exhibits an increase in resource abundance (due to resource production) while the consumer densities are still low. Note that the model assumes that resource production is higher in habitat B. During that initial phase, the mean trait increases in habitat A and decreases in habitat B. In this phase, the dynamics of $\bar{z}^A$ is dominated by the first line in equation (37). Once the peak in resource abundance is reached, resource consumption brings the densities of consumers up and the resource abundance down to habitat-specific equilibrium values. As the resource abundance decreases, the selective advantage of the more prudent morph increases and the rapacious morph is eventually competitively excluded in both habitats, as shown by the decrease in habitat variances. At this point, the term between brackets in the first line of equation (37) becomes zero, and the dynamics of $\bar{z}^A$ are then entirely driven by the second line. The population is now quasi monomorphic and we have

$$\frac{\mathrm{d}\bar{z}^A}{\mathrm{d}t} = V_1 [c_1^A \rho_A'(\bar{z}_i) + c_1^B \rho_B'(\bar{z}_i)], \tag{38}$$

so that the mean trait increases in the direction of the slopes of the growth rates, weighted by the class reproductive values in each habitat. In our simulations, we assume $d(z) = 1 + z$ and $b(z) = b_0 z/(1 + z)$, which leads to the following relationship for the equilibrium value:

$$\bar{z}_{\mathrm{eq}}^A = \sqrt{b_0\left(c_1^A \frac{S^A}{1 + \tau S^A} + c_1^B \frac{S^B}{1 + \tau S^B}\right)} - 1. \tag{39}$$

This long-term equilibrium value is indicated by the gray dotted lines in figure 6*B* and 6*C*, and we see that the slow increase of the mean trait toward this value unfolds on a much longer timescale than the fast out-of-equilibrium dynamics. Note that in figure 6 the results of simulations of the full model are also given (circles), showing that our approximation very accurately captures the short- and long-term dynamics of the ecological variables and of the habitat-specific moments.

Figure 6 assumes that the initial standing variation in the population is large. This corresponds to what is called strong selection in invasion analyses (i.e., the two morphs have different means). It is interesting to compare the results with the dynamics predicted when the standing variation in the population is small, that is, when the morph means are initially close (e.g., weak selection). In this case, figure S8 shows that following a negligible transient increase, the mean trait in each habitat slowly decreases until the equilibrium value is reached. This is easily understood

from equation (37) because when $\bar{z}_1 - \bar{z}_2$ is initially small, only the slow dynamics captured by the second line drive the dynamics of the habitat mean.

Although this rapid analysis of a toy model is by no means an extensive exploration of its behavior, it illustrates the value of our approach when analyzing eco-evolutionary dynamics across different timescales. In particular, equation (37) bridges the gap between fast evolutionary dynamics in nonequilibrium population (typically analyzed in ecological and quantitative genetics models) and slow evolutionary dynamics in populations that have reached an ecological attractor (typically analyzed using adaptive dynamics).

Discussion

We have developed a novel theoretical framework to model the eco-evolutionary dynamics of polymorphic class-structured populations. Our approach leads to dynamical equations that allow us to bridge the gap between quantitative genetics approaches, which are typically interested in short-term transient dynamics under substantial standing variation, and adaptive dynamics approaches, which focus on long-term eco-evolutionary statics under mutation-limited evolution. Our analysis makes two key contributions. First, we extend the recently developed oligomorphic approximation (Sasaki and Dieckmann 2011) to class-structured populations. Since class structure is a major feature of natural biological populations, this allows the method to be applied to a broad range of ecological scenarios, taking into account individual differences in state, including age, spatial location, infection or physiological status, and species. Second, we combine this approximation with recent theory on reproductive values to obtain a lower-dimensional approximation of the eco-evolutionary dynamics of multimorph-structured populations. The combination of these two approximations allows us to obtain compact analytical expressions for the dynamics of multimodal trait distributions in structured populations under density- and frequency-dependent selection. These analytical results are biologically insightful, as they highlight how the quality and quantity of individuals in different classes affect the eco-evolutionary dynamics.

At a general level, our theoretical framework lies at the intersection of population genetics, quantitative genetics, and adaptive dynamics. First, as in population genetics, it predicts how the frequencies of interacting morphs change over time but explicitly takes into account eco-evolutionary feedbacks. Second, we also describe the dynamics of the mean and variance of the trait distribution of each morph. This is reminiscent of moment methods typically used in quantitative genetics (Barton and Turelli 1987, 1991; Turelli and Barton 1990), but our approach effectively extends these tools to multimodal distributions, frequency-dependent selection, and a broad range of ecological scenarios. Third, while our result for the dynamics of the mean takes the form of Lande's univariate theorem (Lande 1976, 1979, 1982; Barfield et al. 2011), we also track the dynamics of genetic variance and describe how initially unimodal distributions can split into different modes as a result of frequency-dependent selection. This effectively bridges the gap between quantitative genetics and adaptive dynamics to provide a more complete understanding of the evolution of quantitative traits.

Our approach broadens the scope of classic quantitative genetics theory to examine the dynamics of multimode distributions and a wider range of ecological feedbacks. Classical quantitative genetics methods are typically restricted to unimodal character distributions. However, multimodal distributions are a very common outcome when frequency dependence causes disruptive selection, as often occurs when ecological feedbacks are taken into account in evolutionary models. The possibility to handle disruptive selection has been a landmark of adaptive dynamics, but it relies on the assumption that evolution is mutation limited, so that the only source of variation in the population comes from rare mutations. Our approach relaxes these assumptions and allows us to describe the joint effect of mutation and substantial standing variation on the eco-evolutionary dynamics. Although adaptive dynamics provides tools to study evolution in polymorphic resident populations (e.g., after branching; Geritz et al. 1998; Kisdi 1999; Durinx et al. 2008), the resulting analysis is often difficult and restricted to potential evolutionary end points. In contrast, our dynamical approach makes it possible to track the joint dynamics of ecological densities and of multimodal trait distributions.

While these technical advances were already present in Sasaki and Dieckmann's (2011) original article, our extension to class structure makes our analysis directly applicable to a broad range of biological scenarios where individuals differ because of nongenetic factors such as age, physiological status, or spatial location. A drawback of this increased realism is that it inflates the number of ecological and genetic variables we need to track. We therefore apply recent theory on reproductive values (Lion 2018*a*, 2018*b*; Priklopil and Lehmann 2020) to simplify the oligomorphic analysis and obtain a compact description of how the morph-level trait distributions change over time when there are demographic transitions between classes. The key idea is to define a weighted trait distribution that gives us a way of examining how selection acts on a particular morph across all the classes (Fisher 1930; Taylor and Frank 1996; Frank 1998; Rousset 2004; Lehmann and Rousset 2014; Lion 2018*a*). For the dynamics of the mean trait of a morph, the result takes the form of the structured extension of Lande's theorem (see also Barfield et al. 2011), but we also provide a new description of the dynamics of morph variances.

Application of the method to the simplified two-class case gives insight into how stabilizing and disruptive selection are impacted by class frequencies and reproductive values and shows when directional selection will impact disruptive selection. As such, we provide a very general tractable framework for a more complete eco-evolutionary analysis of class-structured models.

Reproductive value is an important concept in evolutionary ecology, which is ubiquitous whenever one has to deal with structured populations and provides a biologically intuitive measure of quality (Fisher 1930; Rousset 1999, 2004; Grafen 2006; Lehmann and Rousset 2014; Gardner 2015; Lion 2018*a*). As such, a limitation of previous analyses of two-habitat migration-selection models was that they did not make a clear connection between the predictions and the concept of reproductive value. Our example 1 thus provides a conceptually useful complement to the analyses of Débarre et al. (2013), Meszéna et al. (1997), Mirrahimi and Gandon (2020), and Ronce and Kirkpatrick (2001), as it provides clear interpretations of directional and disruptive selection in terms of the reproductive values of the two habitats. We also show that our reproductive value–weighted approximation accurately predicts the numerical simulations of the full system, with or without mutation-selection balance. In addition, we show that the condition for disruptive selection takes a very simple form and can be summed up through a measure of habitat differentiation that depends on the class reproductive values. Nonetheless, it would be particularly interesting to couple our approach with the Hamilton-Jacobi framework introduced by Mirrahimi and Gandon (2020), which accurately predicts the equilibrium trait distribution even when the mutation rate is large but does not track the dynamics of the distribution over time.

Another important implication of our results is that they allow us to analyze the eco-evolutionary dynamics across different timescales. As such, our approach is very relevant to the current revival of interest on the timescales of ecological and evolutionary processes, as it can be used to examine the role of "fast evolution" when this is fueled by a large standing variation at the population level. In our equations, this corresponds to morphs with very different trait means. As shown in our example 3, our analysis allows us to shed light on the interplay between fast and slow eco-evolutionary processes and to examine the evolutionary consequences of nonequilibrium dynamics. This has broad implications, as rapid or short-term evolution is a crucial process in conservation biology and epidemiology. For instance, our resource-consumer example predicts transient selection for increased resource exploitation, which is similar to a classic prediction that virulent pathogen strains should be favored at the start of an epidemic and more prudent strains should be selected for at endemic equilibrium (Lenski and May 1994; Day and Proulx 2004; Day and Gandon 2007; Berngruber et al. 2013). Hence, our approach could be used to generate predictions for the evolutionary consequences of nonequilibrium processes, such as disease seasonality (Altizer et al. 2006; Ferris and Best 2018; Lion and Gandon 2021), or repeated epidemics driven by antigenic escape (Sasaki et al. 2022). More generally, extensions of our approach could be used to better understand how environmental fluctuations affect disruptive selection and polymorphism, as this represents a fundamental but currently understudied research area (but for an adaptive dynamics treatment, see Svardal et al. 2015).

Our formalism has strong links with the current interest in clarifying the connection between adaptive dynamics and quantitative genetics models (Abrams 2001; Day 2005; Lion 2018*c*) and analyzing eco-evolutionary dynamics at different timescales (see, e.g., Bassar et al. 2021). This has led to various theoretical developments that employ very similar ideas to those we use here and focus on fundamental ecological questions such as transient dynamics (Day and Proulx 2004), community stability (Barabás and D'Andrea 2016), multivariate traits (Mullon and Lehmann 2019), demographic stochasticity (Débarre and Otto 2016), and periodic environments (Lion and Gandon 2021). Compared with these other works, a key advantage of the morph decomposition we employ is that it makes it easier to consider non-Gaussian distributions at the population level by approximating the population-level moments in terms of morph moments, but it would be particularly interesting to couple our approach with these other technical frameworks.

At a biological level, we expect our approach will allow us to deepen our understanding of the processes that generate and maintain diversity in traits. Although the number of morphs can be arbitrarily chosen, it makes sense to use biological principles to guide this choice. For instance, in our two-habitat model, we typically expect that at most two different morphs will coexist because of the competitive exclusion principle. In practice, a scenario where the number of morphs is insufficient can be quickly identified in numerical simulations, as it corresponds to a situation where at least one morph variance diverges to infinity. At a more conceptual level, the number of morphs in our approach is linked to the dimension of the environmental feedback, which sets an upper limit to diversity (Meszéna et al. 2006; Metz et al. 2008; Lion and Metz 2018).

We illustrate the application of the approach using two-habitat migration-selection models, but this can be broadened to examine fundamental processes, such as more general forms of stage structure, species interactions, and speciation. For instance, the approach can be used to determine the time required until a population diversifies under frequency-dependent disruptive selection, which for asexually reproducing species is the waiting time until adaptive

speciation. Additional insights will come from both ecological extensions (such as assortative mating) and, in particular, genetic extension (such as multilocus inheritance, recombination, diploidy, and random genetic drift). In addition, while we have focused on the evolution of single traits, an important extension of our work would consider multivariate traits (e.g., for a quantitative genetics treatment without class structure, see Mullon and Lehmann 2019; for a two-trait extension of the oligomorphic approximation, see Sasaki et al. 2022). In particular, plastic traits (i.e., traits that are not expressed in all classes) could be relatively easily taken into account in a multivariate extension of the framework we present here.

To sum up, we think our analytical approach will allow for a better understanding of the role of ecological feedbacks, frequency-dependent selection, and density-dependent selection in nature and has the potential to facilitate a tighter integration between eco-evolutionary theory and empirical data. At a technical level, our approach moves the field from focusing either on unimodal character distributions, often taken in models of quantitative genetics theory, or on negligible within-morph variance, which is often assumed in models of adaptive dynamics. At a biological level, it has considerable potential to advance our understanding of the ecological factors driving the evolution and maintenance of diversity, which remains an important empirical and theoretical challenge in multiple fields and contexts.

Note

Readers of this article may be interested in the work by Wickman et al. (2021), who independently derived a related formalism to analyze eco-evolutionary dynamics in structured populations.

Acknowledgments

We thank two anonymous reviewers for very constructive and detailed comments. This study was supported by Agence Nationale de la Recherche (ANR) JCJC grant ANR-16-CE35-0012-01 to S.L., grants R01 GM122061-03 and NSF-DEB-2011109 to M.B., and the ESB Cooperation Program, Graduate University for Advanced Studies, SOKENDAI. This work was initiated during a visit by S.L. and M.B. to SOKENDAI in January 2019.

Statement of Authorship

S.L., M.B., and A.S. conceived of the project. S.L. and A.S. conducted the theoretical development and model analysis. S.L. was responsible for the numerical simulations and figures and wrote the first draft of the manuscript. S.L., M.B., and A.S. contributed to subsequent versions.

Data and Code Availability

The Mathematica notebooks and R files used to run the numerical simulations and generate the figures are accessible from Zenodo (https://doi.org/10.5281/zenodo.6334817).

APPENDIX A

Oligomorphic Approximation

From equation (9), it is straightforward to derive the dynamics of the within-class trait distributions $\phi^k(z,t) = n^k(z,t)/n^k(t)$. We obtain, dropping the dependency on time for simplicity,

$$\frac{\mathrm{d}\phi^k(z)}{\mathrm{d}t} = \sum_j \frac{f^j}{f^k}[r^{kj}(z)\phi^j(z) - \phi^k(z)\bar{r}^{kj}]. \tag{A1}$$

To derive the oligomorphic approximation for our class-structured population model, we proceed as in equation (6) of Sasaki and Dieckmann (2011) and define the dynamics of the frequencies f_i^k so that individuals with phenotype z have the same per capita growth rate in a given class, independently of which morph they belong to. This translates into

$$\frac{1}{f_i^k\phi_i^k(z)}\frac{\mathrm{d}(f_i^k\phi_i^k(z))}{\mathrm{d}t} = \frac{1}{\phi^k(z)}\frac{\mathrm{d}\phi^k(z)}{\mathrm{d}t}, \tag{A2}$$

which can be rewritten as

$$\frac{\mathrm{d}(f_i^k\phi_i^k(z))}{\mathrm{d}t} = \frac{f_i^k\phi_i^k(z)}{\phi^k(z)}\frac{\mathrm{d}\phi^k(z)}{\mathrm{d}t}. \tag{A3}$$

Integrating over z and using equation (A1) yields

$$\frac{\mathrm{d}f_i^k}{\mathrm{d}t} = f_i^k\sum_j \frac{f^j}{f^k}\int r^{kj}(z)\frac{\phi^j(z)}{\phi^k(z)}\phi_i^k(z)\,\mathrm{d}z - f_i^k\sum_j \bar{r}^{kj}\frac{f^j}{f^k}.$$

To simplify this equation, we use the following equality, which simply means that if individuals with phenotype z are, say, twice more abundant in class j than class k, this ratio is preserved irrespective of the morph to which they belong:

$$\frac{\phi^j(z)}{\phi^k(z)} = \frac{f_i^j\phi_i^j(z)}{f_i^k\phi_i^k(z)}. \tag{A4}$$

In section S1 of the supplemental PDF, we show that equation (A4) naturally follows from assumption (A2). Plugging equation (A4) into the dynamics of frequencies above then leads to the first part of equation (11):

$$\frac{\mathrm{d}f_i^k}{\mathrm{d}t} = \sum_j \frac{f^j}{f^k}(f_i^j\bar{r}_i^{kj} - f_i^k\bar{r}^{kj}). \tag{A5}$$

With only one class, we recover equation (7) in Sasaki and Dieckmann (2011). The second part of equation (11) can then be obtained by plugging approximations (6) and (7) into equation (A5).

Similarly, to calculate the dynamics of $\phi_i^k(z)$, we rearrange equation (A2) as

$$\frac{\mathrm{d}\phi_i^k(z)}{\mathrm{d}t} = \frac{\phi_i^k(z)}{\phi^k(z)}\frac{\mathrm{d}\phi^k(z)}{\mathrm{d}t} - \phi_i^k(z)\left(\frac{1}{f_i^k}\frac{\mathrm{d}f_i^k}{\mathrm{d}t}\right).$$

Using equations (A1), (A4), and (A5) then yields after some rearrangement

$$\frac{\mathrm{d}\phi_i^k(z)}{\mathrm{d}t} = \sum_j \frac{f_i^j f^j}{f_i^k f^k}\left[\phi_i^j(z) r^{kj}(z) - \phi_i^k(z)\bar{r}_i^{kj}\right]. \tag{A6}$$

With a single class, we recover equation (8) in Sasaki and Dieckmann (2011).

APPENDIX B

Dynamics of Class-Specific Morph Moments

Equation (A6) can be multiplied by z or $(z - \bar{z}_i^k)^2$ and integrated to obtain the dynamics of the morph means and variances, respectively. For the morph means, we obtain

$$\begin{aligned}\frac{\mathrm{d}\bar{z}_i^k}{\mathrm{d}t} &= \sum_j \frac{f_i^j f^j}{f_i^k f^k}\underset{\phi_i^j}{\mathrm{Cov}}(z, r^{kj}(z)) \\ &\quad + \sum_j \frac{f_i^j f^j}{f_i^k f^k}\bar{r}_i^{kj}(\bar{z}_i^j - \bar{z}_i^k),\end{aligned} \tag{B1}$$

where the covariances are taken over the distributions $\phi_i^j(z, t)$ and take the form

$$\underset{\phi_i^j}{\mathrm{Cov}}(z, r^{kj}(z)) = \int (z - \bar{z}_i^j)(r^{kj}(z) - \bar{r}_i^{kj})\phi_i^j(z)\,\mathrm{d}z.$$

Equation (B1) is a morph-specific version of equation (3) in Lion (2018*a*). Using the Taylor expansion (6), we have

$$\begin{aligned}\underset{\phi_i^j}{\mathrm{Cov}}(z, r^{kj}(z)) &= \int \xi_i^j\left(\xi_i^j\frac{\partial r^{kj}}{\partial z}\bigg|_{z=\bar{z}_i^j} + \frac{1}{2}((\xi_i^j)^2 - V_i^j)\frac{\partial^2 r^{kj}}{\partial z^2}\bigg|_{z=\bar{z}_i^j}\right)\phi_i^j(z)\,\mathrm{d}z \\ &= V_i^j\frac{\partial r^{kj}}{\partial z}\bigg|_{z=\bar{z}_i^j} + \frac{1}{2}T_i^j\frac{\partial^2 r^{kj}}{\partial z^2}\bigg|_{z=\bar{z}_i^j} + O(\varepsilon^4),\end{aligned} \tag{B2}$$

where T_i^j is the third central moment of $\phi_i^j(z)$, which we neglect in the following (assuming ϕ_i^j is symmetric). Substituting equations (B2) and (7) into equation (B1), we then obtain

$$\begin{aligned}\frac{\mathrm{d}\bar{z}_i^k}{\mathrm{d}t} = \sum_j \frac{f_i^j f^j}{f_i^k f^k}&\left[(\bar{z}_i^j - \bar{z}_i^k)r^{kj}(\bar{z}_i^j) + V_i^j\frac{\partial r^{kj}}{\partial z}\bigg|_{z=\bar{z}_i^j}\right. \\ &\left. + \frac{1}{2}(\bar{z}_i^j - \bar{z}_i^k)V_i^j\frac{\partial^2 r^{kj}}{\partial z^2}\bigg|_{z=\bar{z}_i^j}\right] \\ &+ O(\varepsilon^4).\end{aligned}$$

Keeping only terms up to the second order in ε, we obtain equation (14).

For the morph variances, defined as $V_i^k = \int (\xi_i^k)^2\phi_i^k(z)\,\mathrm{d}z$, we have, using equations (A6), (6) and (7),

$$\begin{aligned}\frac{\mathrm{d}V_i^k}{\mathrm{d}t} = \sum_j \frac{f_i^j f^j}{f_i^k f^k}&\left[\int (\xi_i^k)^2\left(r^{kj}(\bar{z}_i^j) + \xi_i^j\frac{\partial r^{kj}}{\partial z}\bigg|_{z=\bar{z}_i^j} + \frac{1}{2}(\xi_i^j)^2\frac{\partial^2 r^{kj}}{\partial z^2}\bigg|_{z=\bar{z}_i^j}\right)\phi_i^j(z)\,\mathrm{d}z\right. \\ &\left. - V_i^k\left(r^{kj}(\bar{z}_i^j) + \frac{1}{2}V_i^j\frac{\partial^2 r^{kj}}{\partial z^2}\bigg|_{z=\bar{z}_i^j}\right)\right] + O(\varepsilon^5).\end{aligned}$$

We can further simplify with the following relationships:

$$\begin{aligned}\int (\xi_i^k)^2\phi_i^j(z)\,\mathrm{d}z &= \int (\xi_i^j + \bar{z}_i^j - \bar{z}_i^k)^2\phi_i^j(z)\,\mathrm{d}z \\ &= V_i^j + (\bar{z}_i^j - \bar{z}_i^k)^2, \\ \int (\xi_i^k)^2\xi_i^j\phi_i^j(z)\,\mathrm{d}z &= \int (\xi_i^3 + 2(\bar{z}_i^j - \bar{z}_i^k)(\xi_i^j)^2 \\ &\quad + (\bar{z}_i^j - \bar{z}_i^k)^2\xi_i^j)\phi_i^j(z)\,\mathrm{d}z \\ &= T_i^j + 2(\bar{z}_i^j - \bar{z}_i^k)V_i^j, \\ \int (\xi_i^k)^2(\xi_i^j)^2\phi_i^j(z)\,\mathrm{d}z &= \int (\xi_i^4 + 2(\bar{z}_i^j - \bar{z}_i^k)(\xi_i^j)^3 \\ &\quad + (\bar{z}_i^j - \bar{z}_i^k)^2(\xi_i^j)^2)\phi_i^j(z)\,\mathrm{d}z \\ &= Q_i^j + 2(\bar{z}_i^j - \bar{z}_i^k)T_i^j + (\bar{z}_i^j - \bar{z}_i^k)^2V_i^j.\end{aligned}$$

This yields equation (15), again using the assumption that the morph distribution ϕ_i^j is symmetric so that $T_i^j = 0$.

APPENDIX C

Dynamics of Population-Level Morph Moments

The derivations in appendix B yield dynamical equations for the class-specific morph moments. Depending on the question of interest, it may be useful to focus on the population-level morph moments, averaged over all classes. This can be done in two ways.

Unweighted Morph Distribution

A natural way is to introduce the following average distribution, which corresponds to the unweighted arithmetic mean of the class-specific distributions (Lion 2018*a*):

$$\phi_i(z) = \sum_k \phi_i^k(z)u_i^k,$$

where $u_i^k = f_i^k f^k / f_i$ and $f_i = \sum_k f_i^k f^k$ is the total frequency of morph i in the population. Integrating over z leads to a relationship between morph means, $\bar{z}_i = \sum_k \bar{z}_i^k u_i^k$, from which the following equation can be derived:

$$\begin{aligned}\frac{\mathrm{d}\bar{z}_i}{\mathrm{d}t} &= \sum_j u_i^j\underset{\phi_i^j}{\mathrm{Cov}}\left(z, \sum_k r^{kj}(z)\right) \\ &\quad + \sum_j u_i^j\left(\sum_k \bar{r}_i^{kj}\right)(\bar{z}_i^j - \bar{z}_i).\end{aligned} \tag{C1}$$

This is the morph-specific equivalent of equation (2) in Lion (2018*a*), and an oligomorphic approximation of equation (C1) can be derived using approximations (6) and (7). A similar equation can be derived for the dynamics of the morph variance, $V_i = \int (z - \bar{z}_i)^2 \phi_i(z)\, dz$.

Reproductive Value–Weighted Morph Distribution

In equation (C1), the dynamics of $\bar{z}_i$ depends on the moments of the class-specific distributions $\phi_i^j(z)$. Our goal here is to find a meaningful way to summarize the dynamics using only the moments of the population-level morph distribution $\phi_i(z)$.

There are two equivalent ways to do this. The first approach applies the method of Lion (2018*b*) at the morph level and uses a quasi-equilibrium approximation of the phenotypic differentiations $\bar{z}_i^k - \bar{z}_i$ to simplify equation (C1). This is summarized in section S2 of the supplemental PDF. The second, simpler approach is to calculate the moments of the reproductive value–weighted distribution, as in Lion (2018*a*), but applied at the morph level. The time-dependent reproductive values satisfy equation (13), and the reproductive value–weighted morph distribution is $\tilde{\phi}_i(z) = \sum_k c_i^k \phi_i^k(z)$, where $c_i^k = v_i^k u_i^k$. Following Lion (2018*a*), we obtain the following Price equation:

$$\frac{d\tilde{z}_i}{dt} = \sum_j \sum_k v_i^k \operatorname*{Cov}_{\phi_i^j}(z, r^{kj}(z)) u_i^j. \tag{C2}$$

Equation (C2) is valid irrespective of the shape of the morph distribution. Comparing equations (C1) and (C2) shows that when there is no covariance between the trait and the transition rates (i.e., when the covariance terms are zero), the reproductive value–weighted average $\tilde{z}_i$ does not change while the unweighted average $\bar{z}_i$ can still change because of between-class transitions. Hence, reproductive value weighting allows us to capture the notion that there should be no evolutionary change in a neutral model. Moreover, the dynamics of $\tilde{z}_i$ are always $O(\varepsilon^2)$, so that $\tilde{z}_i$ is a slow variable.

If the morph distribution is sufficiently narrow, we can approximate the covariance terms in equations (C1) and (C2) using equation (B2). Both the quasi-equilibrium and the reproductive value approaches then lead to the following equation:

$$\frac{d\tilde{z}_i}{dt} = \sum_j V_i^j \sum_k v_i^k \left.\frac{\partial r^{kj}}{\partial z}\right|_{z=\bar{z}_i^j} u_i^j + O(\varepsilon^4). \tag{C3}$$

Hence, for narrow morph distributions, the morph mean and the reproductive value–weighted morph mean have the same dynamics on the slow manifold characterized by $\bar{\mathbf{R}}\mathbf{n} = \bar{\mathbf{R}}\mathbf{f} = \bar{\mathbf{R}}_i \mathbf{u}_i = \mathbf{v}_i^{\top} \bar{\mathbf{R}}_i = \mathbf{0}$.

Equation (C3) is a frequency-dependent and polymorphic version of equation (8) in Barfield et al. (2011). Importantly, the RHS of equation (C3) still depends on the class-specific moments $\bar{z}_i^j$ and V_i^j. However, after relaxation on the reproductive value space, the quantities $\bar{z}_i^k - \tilde{z}_i$ and $V_i^k - \tilde{V}_i$ will be $O(\varepsilon^2)$ and $O(\varepsilon^4)$, respectively, under the oligomorphic approximation (see sec. S3 of the supplemental PDF). Hence, to leading order, we can replace the class-specific morph means and variances by the corresponding moments of the reproductive value–weighted distribution. This substitution thus introduces a small error, but it will be quantitatively acceptable as long as the morph variances remain small. This will notably be the case near evolutionary end points under stabilizing selection, but our simulations show that the approximation is also accurate away from evolutionarily singularities. With this last approximation, we obtain equation (29).

We can also calculate the dynamics of the morph variances, either using a quasi-equilibrium approach (as shown in sec. S6 of the supplemental PDF for a two-class model) or by calculating the dynamics of the reproductive value–weighted morph variances $\tilde{V}_i$. This latter approach yields the following Price equation:

$$\frac{d\tilde{V}_i}{dt} = \sum_j \sum_k v_i^k \operatorname*{Cov}_{\phi_i^j}((z - \tilde{z}_i)^2, r^{kj}(z)) u_i^j. \tag{C4}$$

The quadratic term in the covariance can be rewritten using the morph mean $\bar{z}_i^j$ as follows: $(z - \tilde{z}_i)^2 = (z - \bar{z}_i^j)^2 + 2(z - \bar{z}_i^j)(\bar{z}_i^j - \tilde{z}_i) + (\bar{z}_i^j - \tilde{z}_i)^2$. We can use this decomposition to rewrite equation (C4) as

$$\begin{aligned}\frac{d\tilde{V}_i}{dt} = &\sum_j \sum_k v_i^k \operatorname*{Cov}_{\phi_i^j}((z - \bar{z}_i^j)^2, r^{kj}(z)) u_i^j \\ &+ 2 \sum_j \sum_k v_i^k \operatorname*{Cov}_{\phi_i^j}((z - \bar{z}_i^j), r^{kj}(z))(\bar{z}_i^j - \tilde{z}_i) u_i^j.\end{aligned} \tag{C5}$$

Using the Taylor expansion (6) to rewrite the covariance terms, we obtain

$$\begin{aligned}\frac{d\tilde{V}_i}{dt} = &\sum_j \sum_k v_i^k \frac{Q_i^j - (V_i^j)^2}{2} \left.\frac{\partial^2 r^{kj}}{\partial z^2}\right|_{z=\bar{z}_i^j} u_i^j \\ &+ 2 \sum_j V_i^j \sum_k v_i^k \left.\frac{\partial r^{kj}}{\partial z}\right|_{z=\bar{z}_i^j} (\bar{z}_i^j - \tilde{z}_i) u_i^j + O(\varepsilon^5).\end{aligned} \tag{C6}$$

With the Gaussian closure approximation $Q_i^j = 3(V_i^j)^2$ and again using $\bar{z}_i^k - \tilde{z}_i = O(\varepsilon^2)$ and $V_i^k - \tilde{V}_i = O(\varepsilon^4)$, we finally obtain

$$\begin{aligned}\frac{d\tilde{V}_i}{dt} = 2V_i^2 \Bigg[&\frac{1}{2} \sum_j \sum_k v_i^k \left.\frac{\partial^2 r^{kj}}{\partial z^2}\right|_{z=\tilde{z}_i} u_i^j \\ &+ \sum_j \sum_k v_i^k \left.\frac{\partial r^{kj}}{\partial z}\right|_{z=\tilde{z}_i} (\bar{z}_i^j - \tilde{z}_i) u_i^j \Bigg] + O(\varepsilon^5),\end{aligned} \tag{C7}$$

which can be rewritten in matrix form as equation (21).

APPENDIX D

Two-Class Models

Two-class models represent a fundamental tool to analyze structured populations. We therefore develop here how our oligomorphic approximation, together with the reproductive value projection, lead to simple dynamical equations in this case.

Consider a population structured in two classes, A and B. As shown in the general case, the dynamics of morph means and variances are given by the following system of equations:

$$\frac{\mathrm{d}\bar{z}_i}{\mathrm{d}t} = V_i\,\mathbf{v}_i^{\top}\mathbf{S}_i\mathbf{u}_i, \tag{D1a}$$

$$\frac{\mathrm{d}V_i}{\mathrm{d}t} = 2V_i^2[\mathbf{v}_i^{\top}\mathbf{F}_i\mathbf{u}_i + \mathbf{v}_i^{\top}\mathbf{S}_i(\mathbf{d}_i \circ \mathbf{u}_i)]. \tag{D1b}$$

When there are only two classes, it is straightforward to show that

$$\begin{aligned}\frac{\mathrm{d}\bar{z}_i}{\mathrm{d}t} = V_i\Bigg[&v_i^A\frac{\partial r^{AA}}{\partial z}\bigg|_{\bar{z}_i}u_i^A + v_i^B\frac{\partial r^{BA}}{\partial z}\bigg|_{\bar{z}_i}u_i^A\\ &+ v_i^A\frac{\partial r^{AB}}{\partial z}\bigg|_{\bar{z}_i}u_i^B + v_i^B\frac{\partial r^{BB}}{\partial z}\bigg|_{\bar{z}_i}u_i^B\Bigg],\end{aligned} \tag{D2}$$

where the class-reproductive values satisfy the following quasi-equilibrium relationship:

$$c_i^B = v_i^B u_i^B = \frac{r^{AB}(\bar{z}_i)(u_i^B)^2}{r^{BA}(\bar{z}_i)(u_i^A)^2 + r^{AB}(\bar{z}_i)(u_i^B)^2} = 1 - c_i^A, \tag{D3}$$

which can be derived from the equations $\bar{\mathbf{R}}_i\mathbf{u}_i = \bar{\mathbf{R}}_i\mathbf{v}_i = \mathbf{0}$ along with the normalization condition $u_i^A v_i^A + u_i^B v_i^B = 1$ (see sec. S4 of the supplemental PDF).

For the variance dynamics, we similarly have

$$\begin{aligned}\mathbf{v}_i^{\top}\mathbf{F}_i\mathbf{u}_i = \frac{1}{2}\Bigg[&v_i^A\frac{\partial^2 r^{AA}}{\partial z^2}\bigg|_{\bar{z}_i}u_i^A + v_i^B\frac{\partial^2 r^{BA}}{\partial z^2}\bigg|_{\bar{z}_i}u_i^A\\ &+ v_i^A\frac{\partial^2 r^{AB}}{\partial z^2}\bigg|_{\bar{z}_i}u_i^B + v_i^B\frac{\partial^2 r^{BB}}{\partial z^2}\bigg|_{\bar{z}_i}u_i^B\Bigg],\end{aligned} \tag{D4}$$

and for the second term in equation (D1b), which we note $\mathcal{D}_i = \mathbf{v}_i^{\top}\mathbf{S}_i(\mathbf{d}_i \circ \mathbf{u}_i)$, we have

$$\begin{aligned}\mathcal{D}_i = &\left(v_i^A\frac{\partial r^{AA}}{\partial z}\bigg|_{\tilde{z}_i} + v_i^B\frac{\partial r^{BA}}{\partial z}\bigg|_{\tilde{z}_i}\right)(\bar{z}_i^A - \tilde{z}_i)u_i^A\\ &+ \left(v_i^A\frac{\partial r^{AB}}{\partial z}\bigg|_{\tilde{z}_i} + v_i^B\frac{\partial r^{BB}}{\partial z}\bigg|_{\tilde{z}_i}\right)(\bar{z}_i^B - \tilde{z}_i)u_i^B\end{aligned}$$

Because $\tilde{z}_i = c_i^A\bar{z}_i^A + c_i^B\bar{z}_i^B$, we have $\bar{z}_i^A - \tilde{z}_i = c_i^B(\bar{z}_i^A - \bar{z}_i^B)$ and $\bar{z}_i^B - \tilde{z}_i = c_i^A(\bar{z}_i^B - \bar{z}_i^A)$, and therefore

$$\begin{aligned}\mathcal{D}_i = &\left(\frac{\partial r^{AA}}{\partial z}\bigg|_{\tilde{z}_i} + \frac{v_i^B}{v_i^A}\frac{\partial r^{BA}}{\partial z}\bigg|_{\tilde{z}_i}\right)c_i^A c_i^B(\bar{z}_i^A - \bar{z}_i^B)\\ &+ \left(\frac{v_i^A}{v_i^B}\frac{\partial r^{AB}}{\partial z}\bigg|_{\tilde{z}_i} + \frac{\partial r^{BB}}{\partial z}\bigg|_{\tilde{z}_i}\right)c_i^A c_i^B(\bar{z}_i^B - \tilde{z}_i^A),\end{aligned}$$

where we have used the definition $c_i^k = v_i^k u_i^k$. This leads to

$$\begin{aligned}\mathcal{D}_i = &\,c_i^A c_i^B(\bar{z}^B - \bar{z}^A)\\ &\times\left(\frac{\partial r^{AA}}{\partial z}\bigg|_{\tilde{z}_i} + \frac{v_i^B}{v_i^A}\frac{\partial r^{BA}}{\partial z}\bigg|_{\tilde{z}_i} - \frac{\partial r^{BB}}{\partial z}\bigg|_{\tilde{z}_i} - \frac{v_i^A}{v_i^B}\frac{\partial r^{AB}}{\partial z}\bigg|_{\tilde{z}_i}\right).\end{aligned} \tag{D5}$$

More progress can be obtained if we treat the difference $\bar{z}_i^A - \bar{z}_i^B$ as a fast variable (see sec. S2 of the supplemental PDF; Lion 2018*b*). In a two-class model, we have

$$\begin{aligned}\frac{\mathrm{d}\bar{z}_i^A}{\mathrm{d}t} &= V_i^A\frac{\partial r^{AA}}{\partial z}\bigg|_{z=\bar{z}_i^A} + \frac{f_i^B n^B}{f_i^A n^A}r^{AB}(\bar{z}_i^B)(\bar{z}_i^B - \bar{z}_i^A) + O(\varepsilon^4),\\ \frac{\mathrm{d}\bar{z}_i^B}{\mathrm{d}t} &= V_i^B\frac{\partial r^{BB}}{\partial z}\bigg|_{z=\bar{z}_i^B} + \frac{f_i^A n^A}{f_i^B n^B}r^{BA}(\bar{z}_i^A)(\bar{z}_i^A - \bar{z}_i^B) + O(\varepsilon^4).\end{aligned}$$

Using these two equations to calculate the dynamics of $\bar{z}_i^A - \bar{z}_i^B$ and setting the RHS of the resulting equation to zero leads to the following quasi-equilibrium approximation:

$$\begin{aligned}\bar{z}_i^B - \bar{z}_i^A \approx &\frac{u_i^A u_i^B}{r^{AB}(\bar{z}_i^B)(u_i^B)^2 + r^{BA}(\bar{z}_i^A)(u_i^A)^2}\\ &\times\left(V_i^B\frac{\partial r^{BB}}{\partial z}\bigg|_{\bar{z}_i^B} - V_i^A\frac{\partial r^{AA}}{\partial z}\bigg|_{\bar{z}_i^A}\right),\end{aligned} \tag{D6}$$

which can be rewritten using equation (D3) as

$$\bar{z}_i^B - \bar{z}_i^A \approx \sqrt{\frac{c_i^A c_i^B}{r^{AB}(\bar{z}_i^B)r^{BA}(\bar{z}_i^A)}}\left(V_i^B\frac{\partial r^{BB}}{\partial z}\bigg|_{\bar{z}_i^B} - V_i^A\frac{\partial r^{AA}}{\partial z}\bigg|_{\bar{z}_i^A}\right). \tag{D7}$$

We can then use the morph-level closure approximation $\bar{z}_i^k \approx \bar{z}_i$ and $V_i^k \approx V_i$ to finally obtain

$$\begin{aligned}\mathcal{D}_i = &\frac{(c_i^A c_i^B)^{3/2}}{\sqrt{r^{AB}(\bar{z}_i)r^{BA}(\bar{z}_i)}}\left(\frac{\partial r^{AA}}{\partial z}\bigg|_{\bar{z}_i} - \frac{\partial r^{BB}}{\partial z}\bigg|_{\bar{z}_i}\right)\\ &\times\left(\frac{\partial r^{AA}}{\partial z}\bigg|_{\bar{z}_i} + \frac{v_i^B}{v_i^A}\frac{\partial r^{BA}}{\partial z}\bigg|_{\bar{z}_i}\right.\\ &\left. - \frac{\partial r^{BB}}{\partial z}\bigg|_{\bar{z}_i} - \frac{v_i^A}{v_i^B}\frac{\partial r^{AB}}{\partial z}\bigg|_{\bar{z}_i}\right).\end{aligned} \tag{D8}$$

Interestingly, equation (D8) shows that directional selection will have a significant effect on the dynamics of variance if three conditions are met: (1) there is enough differentiation

between the two classes, as measured by the product of class reproductive values $c_i^A c_i^B$; (2) the slopes of the functions r^{AA} and r^{BB} at the morph means are sufficiently different; and (3) the marginal reproductive outputs of A and B individuals are sufficiently different. The latter condition is satisfied when the second bracketed term is nonzero. Note that the ratios v_i^B/v_i^A and v_i^A/v_i^B can be interpreted as conversion factors to evaluate the A and B descendants in the same currency.

Finally, we note that when $\bar{r}^{AB}$ and $\bar{r}^{BA}$ are independent of the trait z, as in our migration-selection models, equation (D8) can be simplified as

$$\mathcal{D}_i = \frac{(c_i^A c_i^B)^{3/2}}{\sqrt{r^{AB}(\bar{z}_i) r^{BA}(\bar{z}_i)}} \left(\frac{\partial r^{AA}}{\partial z}\bigg|_{\bar{z}_i} - \frac{\partial r^{BB}}{\partial z}\bigg|_{\bar{z}_i} \right)^2. \quad \text{(D9)}$$

APPENDIX E

Mutation

The impact of mutation on the oligomorphic dynamics will depend on the specific mutation model one chooses. For simplicity, we assume here that mutation occurs independently of reproduction, at rate μ, and that the mutation effects follow a distribution M_k with mean 0 (mutation has no directional effect) and variance $\sigma_{M,k}^2$. Thus, mutation from phenotype y to phenotype z is determined by a mutation kernel $m^k(z, y)$ in class k, such that for all y, $\int m^k(z, y)\,\mathrm{d}z = 1$, $\int z m^k(z, y)\,\mathrm{d}z = y$ (unbiased mutation), and $\int (z - y)^2 m^k(z, y)\,\mathrm{d}z = \sigma_{M,k}^2$. With these assumptions, the dynamics of the density of morph i individuals, $n_i^k(z) = \phi_i^k(z) n^k$, can be modified as follows:

$$\frac{\mathrm{d}n_i^k(z)}{\mathrm{d}t} \mathrel{+}= \mu \left[\int m^k(z, y) n_i^k(y, t)\,\mathrm{d}y - n_i^k(z, t) \right] n^k(t), \quad \text{(E1)}$$

where the $+=$ notation means that we just add the term on the RHS to the results in the absence of mutation. Note that equation (E1) assumes that mutation does not allow transitions across morphs, which will be satisfied if mutation is sufficiently local and the morphs sufficiently distinct. It is easy to see that if we integrate equation (E1) over z, the mutation term vanishes, and therefore mutation has no effect on the dynamics of the densities $n_i^k(t)$.

From equation (E1), it is straightforward to derive

$$\begin{aligned} \frac{\mathrm{d}\phi_i^k(z)}{\mathrm{d}t} &= \text{RHS of equation (A6)} \\ &\quad + \mu \left[\int m^k(z, y) \phi_i^k(y)\,\mathrm{d}y - \phi_i^k(z) \right], \end{aligned} \quad \text{(E2)}$$

and following the steps in appendix A, we can also show that mutation does not affect the dynamics of morph frequencies.

Multiplying equation (E2) by z and integrating, we obtain

$$\begin{aligned} \frac{\mathrm{d}\bar{z}_i^k(z)}{\mathrm{d}t} &= \text{RHS of equation (14)} \\ &\quad + \mu \left[\int\int z m^k(z, y)\,\mathrm{d}z \phi_i^k(y)\,\mathrm{d}y - \int z \phi_i^k(z)\,\mathrm{d}z \right]. \end{aligned} \quad \text{(E3)}$$

Assuming that mutation is unbiased, so that $y = \int z m^k(z, y)\,\mathrm{d}z$, it follows that the mutation term in equation (E3) vanishes, so that mutation has no impact on the dynamics of morph means.

To calculate the variance dynamics, we multiply equation (E2) by $(z - \bar{z}_i^k)^2$ and integrate to obtain

$$\begin{aligned} \frac{\mathrm{d}\bar{V}_i^k}{\mathrm{d}t} &= \text{RHS of equation (15)} \\ &\quad + \mu \left[\int\int (z - \bar{z}_i^k)^2 m^k(z, y)\,\mathrm{d}z \phi_i^k(y)\,\mathrm{d}y \right. \\ &\quad \left. - \int (z - \bar{z}_i^k)^2 \phi_i^k(z)\,\mathrm{d}z \right] \\ &= \text{RHS of equation (15)} \\ &\quad + \mu \left[\int\int (z - y)^2 m^k(z, y)\,\mathrm{d}z \phi_i^k(y)\,\mathrm{d}y \right. \\ &\quad + 2 \int (y - \bar{z}_i^k) \int (z - y) m^k(z, y)\,\mathrm{d}z \phi_i^k(y)\,\mathrm{d}y \\ &\quad \left. + \int (y - \bar{z}_i^k)^2 \int m^k(z, y)\,\mathrm{d}z \phi_i^k(y)\,\mathrm{d}y - V_i^k \right] \\ &= \text{RHS of equation (15)} + \mu \sigma_{M,k}^2. \end{aligned}$$

Hence, mutation adds the term $V_M^k = \mu \sigma_{M,k}^2$ to the dynamics of morph variances; $V_{M,k}$ is the mutational variance in class k (Kimura 1965; Lande 1975; Sasaki and Dieckmann 2011). Finally, to derive the dynamics of the reproductive value–weighted morph variance $\tilde{V}_i = \sum_i c_i^k V_i^k$, we simply need to add the term $\sum_i c_i^k V_M^k$ to the RHS of equation (C7), which yields equations (20) and (21).

Literature Cited

Abrams, P. A. 2001. Modelling the adaptive dynamics of traits involved in inter- and intraspecific interactions: an assessment of three methods. Ecology Letters 4:166–175.

Abrams, P. A., H. Matsuda, and Y. Harada. 1993. Evolutionarily unstable fitness maxima and stable fitness minima of continuous traits. Evolutionary Ecology 7:465–487.

Altizer, S., A. Dobson, P. Hosseini, P. Hudson, M. Pascual, and P. Rohani. 2006. Seasonality and the dynamics of infectious diseases. Ecology Letters 9:467–484.

Barabás, G., and R. D'Andrea. 2016. The effect of intraspecific variation and heritability on community pattern and robustness. Ecology Letters 19:977–986.

Barfield, M., R. D. Holt, and R. Gomulkiewicz. 2011. Evolution in stage-structured populations. American Naturalist 177:397–409.

Barton, N. H., and M. Turelli. 1987. Adaptive landscapes, genetic distance and the evolution of quantitative characters. Genetical Research 49:157–173.

———. 1991. Natural and sexual selection on many loci. Genetics 127:229–255.

Bassar, R. D., T. Coulson, J. Travis, and D. N. Reznick. 2021. Towards a more precise—and accurate—view of eco-evolution. Ecology Letters 24:623–625.

Berngruber, T. W., S. Lion, and S. Gandon. 2013. Evolution of suicide as a defense strategy against pathogens in a spatially structured environment. Ecology Letters 16:446–453.

Bonamour, S., C. Teplitsky, A. Charmantier, P. A. Crochet, and L. M. Chevin. 2017. Selection on skewed characters and the paradox of stasis. Evolution 71:2703–2713.

Bulmer, M. G. 1992. The mathematical theory of quantitative genetics. Oxford University Press, Oxford.

Crow, J. F., and M. Kimura. 1970. An introduction to population genetics theory. Burgess, Minneapolis.

Day, T. 2005. Modeling the ecological context of evolutionary change: déjà vu or something new? Pages 273–309 *in* K. Cuddington and B. E. Beisnet, eds. Ecological paradigms lost: routes to theory change. Academic Press, Cambridge, MA.

Day, T., and S. Gandon. 2007. Applying population-genetic models in theoretical evolutionary epidemiology. Ecology Letters 10: 876–888.

Day, T., and S. R. Proulx. 2004. A general theory for the evolutionary dynamics of virulence. American Naturalist 163:E40–E63.

Débarre, F., and S. P. Otto. 2016. Evolutionary dynamics of a quantitative trait in a finite asexual population. Theoretical Population Biology 108:75–88.

Débarre, F., O. Ronce, and S. Gandon. 2013. Quantifying the effects of migration and mutation on adaptation and demography in spatially heterogeneous environments. Journal of Evolutionary Biology 26:1185–1202.

Dieckmann, U., and R. Law. 1996. The dynamical theory of coevolution: a derivation from stochastic ecological processes. Journal of Mathematical Biology 34:579–612.

Durinx, M., J. A. J. Metz, and G. Meszéna. 2008. Adaptive dynamics for physiologically structured populations models. Journal of Mathematical Biology 56:673–742.

Ewens, W. J. 2004. Mathematical population genetics. Springer, New York.

Falconer, D. S. 1996. Introduction to quantitative genetics. Longman, Harlow.

Ferris, C., and A. Best. 2018. The evolution of host defence to parasitism in fluctuating environments. Journal of Theoretical Biology 440:58–65.

Fisher, R. A. 1930. The genetical theory of natural selection. Clarendon, Oxford.

Frank, S. A. 1998. Foundations of social evolution. Princeton University Press, Princeton, NJ.

Gardner, A. 2015. The genetical theory of multilevel selection. Journal of Evolutionary Biology 28:305–319.

Geritz, S. A. H., E. Kisdi, G. Meszéna, and J. A. J. Metz. 1998. Evolutionarily singular strategies and the adaptive growth and branching of the evolutionary tree. Evolutionary Ecology 12:35–57.

Grafen, A. 2006. A theory of Fisher's reproductive value. Journal of Mathematical Biology 53:15–60.

———. 2015. Biological fitness and the Price equation in class-structured populations. Journal of Theoretical Biology 373:62–72.

Iwasa, Y., A. Pomiankowski, and S. Nee. 1991. The evolution of costly mate preferences II: the "handicap" principle. Evolution 45:1431–1442.

Kimura, M. 1965. A stochastic model concerning the maintenance of genetic variability in quantitative characters. Proceedings of the National Academy of Sciences of the USA 54:732–736.

Kisdi, E. 1999. Evolutionary branching under asymmetric competition. Journal of Theoretical Biology 197:149–162.

Lande, R. 1975. The maintenance of genetic variability by mutation in a polygenic character with linked loci. Genetical Research 26:221–235.

———. 1976. Natural selection and random genetic drift in phenotypic evolution. Evolution 30:314–334.

———. 1979. Quantitative genetic analysis of multivariate evolution, applied to brain-body size allometry. Evolution 33:402–416.

———. 1982. A quantitative genetic theory of life history evolution. Ecology 63:607–615.

Lehmann, L., and F. Rousset. 2014. The genetical theory of social behaviour. Philosophical Transactions of the Royal Society B 369:20130357.

Lenski, R. E., and R. M. May. 1994. The evolution of virulence in parasites and pathogens: reconciliation between two competing hypotheses. Journal of Theoretical Biology 169:253–265.

Lion, S. 2018*a*. Class structure, demography and selection: reproductive-value weighting in non-equilibrium, polymorphic populations. American Naturalist 191:620–637.

———. 2018*b*. From the Price equation to the selection gradient in class-structured populations: a quasi-equilibrium route. Journal of Theoretical Biology 447C:178–189.

———. 2018*c*. Theoretical approaches in evolutionary ecology: environmental feedback as a unifying perspective. American Naturalist 191:21–44.

Lion, S., and S. Gandon. 2021. Life-history evolution of class-structured populations in fluctuating environments. bioRxiv, https://doi.org/10.1101/2021.03.12.435065.

Lion, S., and J. A. J. Metz. 2018. Beyond R_0 maximisation: on pathogen evolution and environmental dimensions. Trends in Ecology and Evolution 33:75–90.

Meszéna, G., I. Czibula, and S. Geritz. 1997. Adaptive dynamics in a 2-patch environment: a toy model for allopatric and parapatric speciation. Journal of Biological Systems 5:265–284.

Meszéna, G., M. Gyllenberg, L. Pásztor, and J. Metz. 2006. Competitive exclusion and limiting similarity: a unified theory. Theoretical Population Biology 69:68–87.

Metz, J. A. J., S. A. H. Geritz, G. Meszéna, F. J. A. Jacobs, and J. S. van Heerwaarden. 1996. Adaptive dynamics: a geometrical study of the consequences of nearly faithful reproduction. Pages 183–231 *in* S. J. van Strien and S. M. Verduyn Lunel, eds. Stochastic and spatial structures of dynamical systems. North-Holland, Amsterdam.

Metz, J. A. J., S. D. Mylius, and O. Diekmann. 2008. When does evolution optimize? Evolutionary Ecology Research 10:629–654.

Metz, J. A. J., R. M. Nisbet, and S. A. H. Geritz. 1992. How should we define "fitness" for general ecological scenarios? Trends in Ecology and Evolution 7:198–202.

Mirrahimi, S., and S. Gandon. 2020. Evolution of specialization in heterogeneous environments: equilibrium between selection, mutation and migration. Genetics 214:479–491.

Mullon, C., and L. Lehmann. 2019. An evolutionary quantitative genetics model for phenotypic (co)variances under limited dispersal, with an application to socially synergistic traits. Evolution 73:1695–1728.

Mylius, S. D., and O. Diekmann. 1995. On evolutionarily stable life histories, optimization and the need to be specific about density dependence. Oikos 74:218–224.

Ohtsuki, H., C. Rueffler, J. Y. Wakano, K. Parvinen, and L. Lehmann. 2020. The components of directional and disruptive selection in heterogeneous group-structured populations. Journal of Theoretical Biology 507:110449.

Priklopil, T., and L. Lehmann. 2020. Invasion implies substitution in ecological communities with class-structured populations. Theoretical Population Biology 134:36–52.

Rinaldi, S., and M. Scheffer. 2000. Geometric analysis of ecological models with slow and fast processes. Ecosystems 3:507–521.

Ronce, O., and M. Kirkpatrick. 2001. When sources become sinks: migrational meltdown in heterogeneous habitats. Evolution 55:1520–1531.

Rousset, F. 1999. Reproductive value vs sources and sinks. Oikos 86:591–596.

———. 2004. Genetic structure and selection in subdivided populations. Princeton University Press, Princeton, NJ.

Sasaki, A., and U. Dieckmann. 2011. Oligomorphic dynamics for analyzing the quantitative genetics of adaptive speciation. Journal of Mathematical Biology 63:601–635.

Sasaki, A., S. Lion, and M. Boots. 2022. Antigenic escape selects for the evolution of higher pathogen transmission and virulence. Nature Ecology and Evolution 6:51–62.

Svardal, H., C. Rueffler, and J. Hermisson. 2015. A general condition for adaptive genetic polymorphism in temporally and spatially heterogeneous environments. Theoretical Population Biology 99:76–97.

Taylor, P. D. 1990. Allele-frequency change in a class-structured population. American Naturalist 135:95–106.

Taylor, P. D., and S. A. Frank. 1996. How to make a kin selection model? Journal of Theoretical Biology 180:27–37.

Turelli, M., and N. H. Barton. 1990. Dynamics of polygenic characters under selection. Theoretical Population Biology 38:1–57.

Walsh, B., and M. Lynch. 2018. Evolution and selection of quantitative traits. Oxford University Press, Oxford.

Wickman, J., T. Koffel, and C. A. Klausmeier. 2021. A general theoretical framework for trait-based eco-evolutionary dynamics: population structure, intraspecific variation, and community assembly. bioRxiv, https://doi.org/10.1101/2021.10.01.462789.

Associate Editor: Laurent Lehmann
Editor: Erol Akçay

"The American reader will find that some of the characteristic ruminants of his country are well drawn, as in the Rocky Mountain sheep and the musk ox [figured]." From the review of Brehm's *Thierleben* (*The American Naturalist*, 1878, 12:682–685).